UCRL-10747

University of California

Ernest O. Lawrence Radiation Laboratory

TWO-WEEK LOAN COPY

This is a Library Circulating Copy which may be borrowed for two weeks. For a personal retention copy, call Tech. Info. Division, Ext. 5545

ELECTRONIC AND NUCLEAR PROPERTIES OF Er^{171}, Tm^{171}, and Tb^{161}

Berkeley, California

DISCLAIMER

This document was prepared as an account of work sponsored by the United States Government. While this document is believed to contain correct information, neither the United States Government nor any agency thereof, nor the Regents of the University of California, nor any of their employees, makes any warranty, express or implied, or assumes any legal responsibility for the accuracy, completeness, or usefulness of any information, apparatus, product, or process disclosed, or represents that its use would not infringe privately owned rights. Reference herein to any specific commercial product, process, or service by its trade name, trademark, manufacturer, or otherwise, does not necessarily constitute or imply its endorsement, recommendation, or favoring by the United States Government or any agency thereof, or the Regents of the University of California. The views and opinions of authors expressed herein do not necessarily state or reflect those of the United States Government or any agency thereof or the Regents of the University of California.

Research and Development

UCRL-10747
UC-34 Physics
TID-4500 (19th Ed.)

UNIVERSITY OF CALIFORNIA
Lawrence Radiation Laboratory
Berkeley, California

Contract No. W-7405-eng-48

ELECTRONIC AND NUCLEAR PROPERTIES OF Er^{171}, Tm^{171}, AND Tb^{161}

Isaac Maleh

(Ph. D. Thesis)

March 29, 1963

Printed in USA. Price $2.00. Available from the
Office of Technical Services
U. S. Department of Commerce
Washington 25, D.C.

ELECTRONIC AND NUCLEAR PROPERTIES OF Er^{171}, Tm^{171}, AND Tb^{161}

Contents

Abstract v

I. Introduction 1

II. Theory

A. Electronic Structure 2

B. Nuclear Structure 7

C. Hyperfine Structure 16

III. Experimental Technique 21

IV. Experimental Results

A. Thulium-171 37

B. Terbium-161 46

C. Erbium-171 52

Acknowledgments 66

Appendix 67

References 69

ELECTRONIC AND NUCLEAR PROPERTIES OF Er^{171}, Tm^{171}, AND Tb^{161}

Isaac Maleh

Lawrence Radiation Laboratory
University of California
Berkeley, California

March 29, 1963

ABSTRACT

By means of the atomic-beam magnetic resonance flop-in technique, the following new physical constants were measured:

Isotope	Measurements Previous	Measurements New
$_{68}Er^{171}$	$(4f)^{12}(6s)^2$	a = ± 197.0(2.9) Mc
		b = ± 3646(106) Mc
τ = 7.5 h	$^3H_6$, I = 5/2	μ_I(corr) = ± 0.697(48) nm
	[512] 5/2-	Q(uncorr) = ∓ 2.37(20) b
		$\frac{b}{a} > 0$
$_{69}Tm^{171}$	$(4f)^{13}(6s)^2$	a = ± 372.1(5.9) Mc
τ = 1.9 yr	$^2F_{7/2}$, I = 1/2	μ_I(corr) = ± 0.227(5) nm
	[411] 1/2+	
$_{65}Tb^{161}$	$(4f)^8 5d(6s)^2$	I = 3/2
τ = 6.8 days	J = 11/2, 13/2	[411] 3/2

The nuclear magnetic moment and nuclear quadrupole moment were calculated from the Fermi-Segrè relation and from the $\left\langle \frac{1}{r^3} \right\rangle$ value by using other researchers' published values.

All of these nuclei are in the collective model region and can be described by suitable Nilsson state assignments as indicated above. The quadrupole moment of Er^{171} yields a deformation of 0.238(20) which is low compared with those generally found in the rare-earth region; the nuclear magnetic moment of Er^{171} is less than collective-model predictions (perhaps due to uncertainty in g_R). Assuming a reasonable deformation factor for Tm^{171} the collective-model prediction for its nuclear magnetic moment agrees remarkably well with the measured value. The spin and resulting Nilsson state assignment for Tb^{161} agrees with that assumed from its decay scheme.

A detailed description of the technique and a theoretical analysis of each result are presented.

I. INTRODUCTION

Atomic-beam experiments make possible the following measurements:

Angular momentum of the nucleus	($\underset{\sim}{I}$)
Angular momentum of the electrons	($\underset{\sim}{J}$)
Hyperfine interaction constants:	(a) magnetic dipole
	(b) electric quadrupole
Magnetic moment of the nucleus	($\underset{\sim}{\mu}_I$)
Magnetic moment of the electrons	($\underset{\sim}{\mu}_J$).

If good values of $\langle 1/r^3 \rangle$ are available, the nuclear electric quadrupole moment and ∇E at the nucleus can be extracted. The nuclear magnetic moment appears directly only if extreme accuracy exists in the data, and so is usually calculated from "a" and reliable $\langle 1/r^3 \rangle$ values.

This paper will present the theory underlying atomic-beam experiments in general, and describe the particular technique used in obtaining the results mentioned in the abstract. The theory of electronic and nuclear structure will be developed and comparisons will be made with the experimental data.

Standard notation is used throughout the text. The only possibly confusing symbols are "a" and "ξ". The symbol "a" is used as the magnetic-dipole interaction constant and in Sections IV-A and II-B as the decoupling factor in the collective-model nucleus, while "ξ" is used in the spin-orbit term of the Hamiltonian as well as for the ratio $\frac{b}{a}$. Because of their limited use, being forewarned eliminates the confusion.

II. THEORY

A. Electronic Structure

A free atom can be described by the following Hamiltonian:

$$\mathcal{H}_{total} = \mathcal{H}_{nuclear} + \mathcal{H}_{electronic} + \mathcal{H}_{hfs} \tag{2.1}$$

The first term represents the internal energy of the nucleus; since we are only dealing with the nuclear ground state it will not concern us here. The second part has the following form:

$$\mathcal{H}_{electronic} + \mathcal{H}_{hfs} = \sum_{i=1}^{N} \left(\frac{\underset{\sim}{p}_i^2}{2m} - \frac{Ze^2}{r_i} + \xi(r_i)\, \underset{\sim}{\ell}_i \cdot \underset{\sim}{s}_i \right) + \sum_{i>j=1}^{N} \frac{e^2}{r_{ij}} + \mathcal{H}_{hfs} \,. \tag{2.2}$$

The summation runs from 1 to N, which is the total number of electrons present. The first term in (2.2) represents the kinetic energy of the electrons. The second term is the Coulomb potential felt by the ith electron due to the nuclear charge Ze; r_i is the distance from the nucleus to the ith electron. The third term (spin-orbit) represents the energy due to the spin magnetic moment interacting with the magnetic field of the nucleus which, as seen by the electron, is circulating about the electron. The fourth term is the electrostatic potential felt by each electron from all the remaining electrons. The fifth term, the hyperfine-structure Hamiltonian, represents the interaction between the electronic and nuclear system and will be discussed at length later, but for now it will be neglected. It should be noted that (2.2) is nonrelativistic and that some terms have been left out due to their diminutive size; i.e., spin-other orbit, orbit-orbit, etc.

The method used in obtaining energy levels–using only the first four terms of (2.2)–and quantum numbers to describe these levels is presented in Condon and Shortley (CON 35). The technique consists of separating the electronic Hamiltonian into two parts:

$$\mathcal{H}_{\text{electronic}} = \mathcal{H}_0 + \mathcal{H}_{\text{pert}}, \tag{2.3}$$

$$\mathcal{H}_0 = \sum_{i=1}^{N} \left[\frac{\underset{\sim}{p}_i^2}{2m} + U(|r_i|) \right], \tag{2.3a}$$

$$\mathcal{H}_{\text{pert}} = \sum_{i=1}^{N} \xi(r_i)\, \underset{\sim}{\ell}_i \cdot \underset{\sim}{s}_i - \frac{Ze^2}{r_i} - U(|r_i|) + \sum_{i>j=1}^{N} \frac{e^2}{r_{ij}}. \tag{2.3b}$$

The idea is to choose $U(|r_i|)$ so that $\mathcal{H}_{\text{pert}} << \mathcal{H}_0$. This spherically symmetric potential is subject to the following boundary conditions:

$$U(|r_i|) \rightarrow \frac{-Ze^2}{r} + \frac{(N-1)}{p} e^2, \text{ as } r \rightarrow 0, \tag{2.4a}$$

and

$$U(|r_i|) \rightarrow \frac{-e^2}{r}, \text{ as } r \rightarrow \infty. \tag{2.4b}$$

Equation (2.4a) represents the potential felt by an electron that is close enough to the nucleus to see just the nucleus on the inside and all the other electrons surrounding it at a mean distance p $(\frac{1}{p} \approx \Sigma\ 1/r_i)$, while (2.4b) is the potential seen from a nucleus screened by $(N-1)$ electrons.

The choice of $U(|r_i|)$ is made consistent with single electron wave functions (Hartree) or an anti-symmetrized product of such wave functions (Hartree-Foch) (HAR 57). That is, the wave functions are eigenfunctions of the Hamiltonian $\mathcal{H}_0$ and are consistent with the production of $U(|r_i|)$. The use of $\mathcal{H}_0$ as the electronic Hamiltonian yields energy levels–normally separated by hundreds of thousands of wave numbers–which can be described by assigning to each electron a principal quantum number n and an orbital quantum number ℓ. Each ℓ

level can have $2(2\ell+1)$ electrons according to the Pauli principle, and for a given n, ℓ goes from 0 to $(n-1)$. This scheme is called the central-field approximation. The assignment of $n\ell$ to each electron in an atom is known as a configuration. These levels are highly degenerate, but application of $\mathcal{H}_{pert}$ removes a good deal of this.

For the most part, two distinct cases occur in $\mathcal{H}_{pert}$. The first and most common is when the electrostatic interaction is much greater than the spin-orbit term; the second is the reverse situation. If

$$\sum_{i>j=1}^{N} \frac{e^2}{r_{ij}} >> \sum_{i=1}^{N} \xi(r_i)\, \underset{\sim}{\ell}_i \cdot \underset{\sim}{s}_i, \tag{2.5}$$

then the configuration is split into levels denoted by $n\ell\, \underset{\sim}{L}\, \underset{\sim}{S}$, where $\underset{\sim}{L} = \sum_i \underset{\sim}{\ell}_i$ and $\underset{\sim}{S} = \sum_i \underset{\sim}{s}_i$. This is a Russell-Saunders coupling (CON 35), in which the orbital angular momentum of each electron couples to a total electronic orbital angular momentum, and similarly for the spin of each electron. Each L, S level is called a term and they are $[(2L+1)(2S+1)]$-fold degenerate. The energy separation of different terms is of the order of 10 000 cm^{-1}. Now if the spin-orbit term is included in $\mathcal{H}_{pert}$, then each term level is split into different J states, J being the total electronic angular momentum. These levels are $(2J+1)$-fold degenerate.

$$\underset{\sim}{J} = \underset{\sim}{L} + \underset{\sim}{S} \text{ (vector sum).} \tag{2.6}$$

If the inequality in (2.5) is reversed, i.e.,

$$\sum_{i>j=1}^{N} \frac{e^2}{r_{ij}} << \sum_{i=1}^{N} \xi(r_i)\, \underset{\sim}{\ell}_i \cdot \underset{\sim}{s}_i, \tag{2.7}$$

one has the case of j-j coupling:

$$\underset{\sim}{J} = \sum_i \underset{\sim}{j}_i , \qquad \underset{\sim}{j}_i = \underset{\sim}{\ell}_i + \underset{\sim}{s}_i , \tag{2.8}$$

and the electrostatic interaction tends to modify these $n\ell\underset{\sim}{J}$ levels.

Figure II-1 illustrates the usual energy-level scheme for an atom. There exists an empirical rule, Hund's rule (H1), to determine the ground-state "term" of an atom: (H1) The ground-state term is obtained by arranging the unpaired electrons to give the maximum $\underset{\sim}{S}$, and with this $\underset{\sim}{S}$ the largest $\underset{\sim}{L}$ consistent with the Pauli principle.

The lowest J state is $|\underset{\sim}{L} + \underset{\sim}{S}|$ if the shell is more than half-filled, and $|\underset{\sim}{L} - \underset{\sim}{S}|$ otherwise. Arguments can be made to support this rule and are presented in the Appendix.

Returning now to configurations, an electron having an $n\ell$ quantum number is said to be in a certain shell. Each shell is $2(2\ell + 1)$-fold degenerate, and different shells posses different energies due to, among other things, their proximity to the nucleus. The energy-level order of these shells in the ground state is the following (SCH 49):

$$1s, 2s, 2p, 3s, 3p, [4s, 3d], 4p, [5s, 4d], 5p, [6s, 4f, 5d], 6p, [7s, 5f, 6d]. \tag{2.9}$$

The shells in brackets denote very similar energy levels. The rare-earth region occurs in the bracket [6s, 4f, 5d], and all the configurations in this region have been determined except Cerium (Z = 58) (MAR 61). The ground-state configurations are determined by matching J and g_J states with theoretical values. What appears to happen in the rare earths is a filling of the 6s shell, and then each additional electron that appears as one goes from Ce (Z = 58) to Lu (Z = 71) goes into the 4f level. The configuration of Ce is still in doubt, although it is very probably a mixture of $(4f)(5d)(6s)^2$ and $(4f)(5d)^2\,6s$ (GER 62).

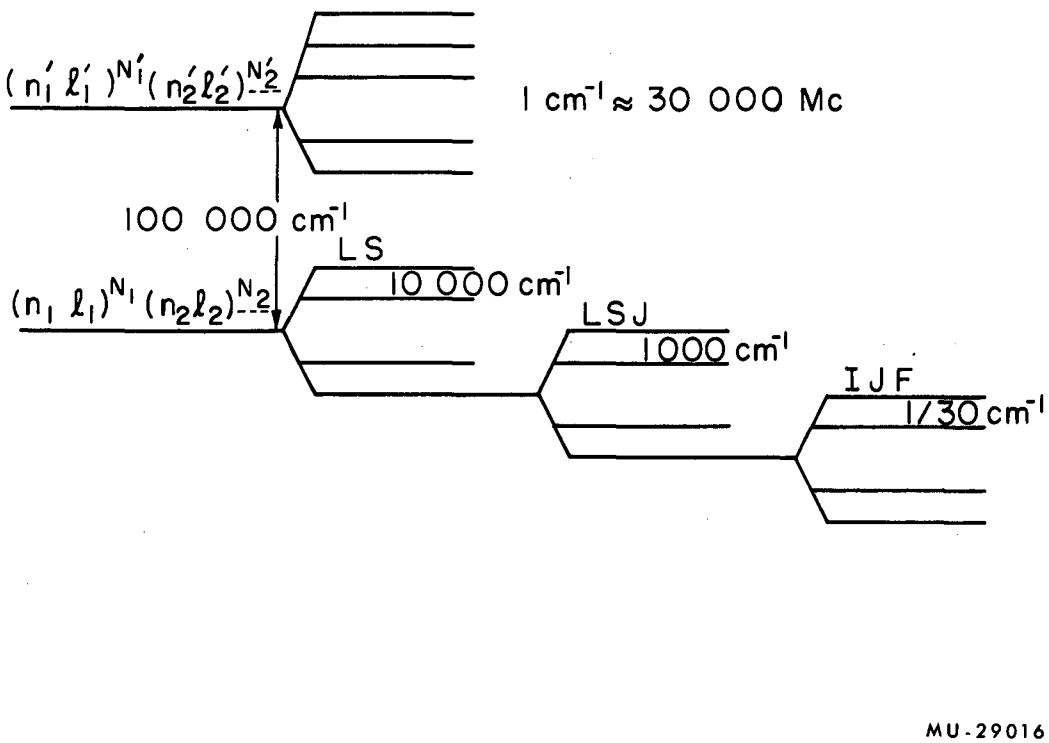

Fig. II-1. The usual energy-level structure of an atom with associated quantum numbers (Russell-Saunders coupling).

B. Nuclear Structure

From the flood of information produced in the past half century on nuclear ground-state properties, the following generalizations can be made:

1. Nuclei with even Z and even N (even-even) have zero spin.
2. Nuclei with odd A have half-integer spin (even Z, odd N, or vice versa).
3. Nuclei with even A have integer spin (odd Z, odd N).
4. Nuclei that contain a so-called magic number of protons and/or neutrons seem particularly stable. These magic numbers are 2, 8, 20, 28, 50, 82, 126. The stability is demonstrated in a number of ways:

   a. Many isotopes (isotones) in existence for nuclei having a "magic" number of protons (neutrons).

   b. Binding-energy measurements indicate substantial changes between say the 50th and 51st proton, indicating the 51st to be loosely bound compared with the 50th.

Because of the mathematical difficulties involved in describing the numerous particles in atomic nuclei, simplified models are sought to explain the above general truths and predict electromagnetic moments of nuclei for comparison with the growing experimental results. Only two of the more common models will be discussed: the shell model and the collective model.

1. Shell Model

The shell model is a single-particle model with a strong spin-orbit coupling term. That is: each nucleon is assumed to move in a static spherically symmetric potential intermediate in shape between a harmonic oscillator and a rectangular well while experiencing an additional potential proportional to the product of its spin and orbital angular momentum $[f(r)\, \underset{\sim}{s} \cdot \underset{\sim}{\ell}\,]$. Without the latter potential, shells are predicted containing 2, 8, 20, 40, 70, 112 nucleons, whereas with the introduction of a spin-orbit term Mayer—and independently, Haxel, Jensen, and Suess (May 55)—were able to account for the observed magic numbers 2, 8, 20, 28, 50, 82, 126. The theory has been very successful thus far in

predicting nuclear spins and parities of odd-A nuclei. The energy levels resulting from such a Hamiltonian are shown in Fig. II-2. Each level is filled with as many neutrons or protons as allowed by the Pauli principle, and the nuclear spin is determined by the last odd particle or particles consistent with the following rules:

(M1) With even Z and even N the spin is zero.

(M2) With even$\binom{Z}{N}$ and odd$\binom{N}{Z}$, the spin is determined by the $\binom{\text{neutrons}}{\text{protons}}$ alone.

(M3) With A odd (condition M2), the nucleons present in odd number will "usually" couple in such a way that the total nuclear spin will be that of the last partially filled orbit.

The resulting predictions are fairly accurate for odd-A nuclei; however, for odd-odd nuclei many conflicts arise. Nordheim (NOR 51) has formulated empirical rules for coupling j_p of the last odd proton to j_n of the last odd neutron:

(N1) If $j_p = \ell_p \pm 1/2$ and $j_n = \ell_n \pm 1/2$, then $I \leq |j_p + j_n|$,

(N2) If $j_p = \ell_p \pm 1/2$ and $j_n = \ell_n \mp 1/2$, then $I = |j_p - j_n|$.

Brennan and Bernstein (BRE 60) have more recently proposed the following rules:

For configurations in which the odd protons and odd neutrons are both particles or both holes:

(B1) $I = |j_p \pm j_n|$ for $j_p = \ell_p \pm 1/2$ and $j_n = \ell_n \pm 1/2$,

(B2) $I = |j_p - j_n|$ for $j_p = \ell_p \pm 1/2$ and $j_n = \ell_n \mp 1/2$,

If j_p or j_n equals 1/2 then $I = |j_p + j_n|$ instead of rule (B1).

For configurations that are mixtures of particles and holes:

(B3) $I = |j_p + j_n - 1|$.

In order to obtain a theoretical prediction for the nuclear magnetic moment and electric quadrupole moment, one must evaluate

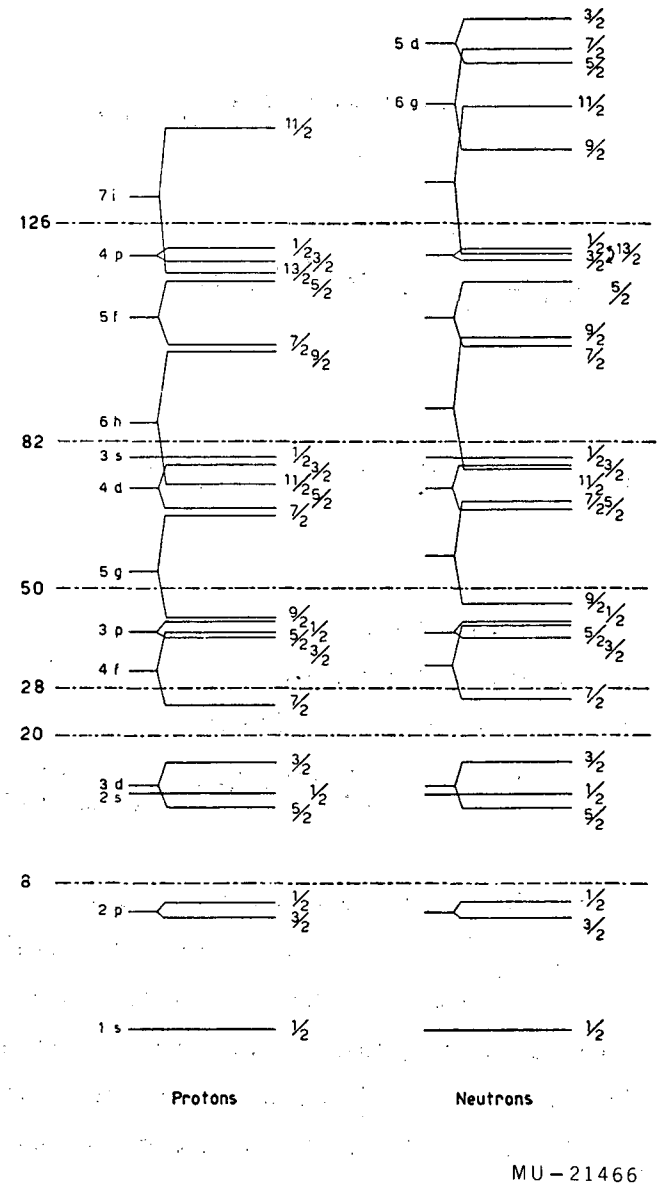

Fig. II-2. Energy-level structure of nucleons according to the shell model, with spin-orbit coupling.

$$\mu = \langle Im | \underset{\sim}{\mu} | Im \rangle_{m = I} \tag{2.10}$$

and

$$Q = \langle Im | \underset{\sim}{Q} | Im \rangle_{m = I}, \tag{2.11}$$

where

$$\underset{\sim}{\mu} = \frac{e\hbar}{2\,Mc} \sum_{k=1}^{A} g_{\ell}^{(k)} \underset{\sim}{\ell}^{(k)} + \frac{e\hbar}{2\,Mc} \sum_{k=1}^{A} g_{s}^{(k)} \underset{\sim}{s}^{(k)}, \text{ erg/G}, \tag{2.12}$$

$$\underset{\sim}{Q} = \sum_{k=1}^{A} g_{\ell}^{(k)} (3\, z_k^2 - r_k^2) \text{ cm}^2, \tag{2.13}$$

I = nuclear spin,

M = mass of a nucleon,

e = charge of proton (esu)

$g_{\ell} = \binom{1}{0}$, $g_s = \binom{5.586}{-3.826}$ for $\binom{\text{protons}}{\text{neutrons}}$.

According to the shell model, every nucleon in the quantum state $|N, \ell, s, j, m_J\rangle$ tries to combine with another in the state $|N, \ell, s, j, -m_J\rangle$, yielding no net magnetic moment. Thus in a nucleus with an even number of protons and on odd number of neutrons, all the protons will combine in pairs and all but the last odd neutron will similarly combine to contribute zero towards the nuclear magnetic moment. The last remaining neutron is the only source of the magnetic moment. Thus, according to whether the last odd particle is a proton or a neutron and whether its spin is parallel or antiparallel to its orbital angular momentum, one obtains the data shown in Table II-1.

Table II-1. Magnets moments of odd-A nuclei according to Shell Model.

Odd particle	$I = j = \ell + 1/2$	$I = j = \ell - 1/2$
Proton	$\mu = j - \frac{1}{2} + \mu_p$ nm	$= j + \frac{j}{j+1}\left(\frac{1}{2} - \mu_p\right)$ nm
Neutron	$= \mu_n$	$= -\frac{j}{j+1}\mu_n$

$$\begin{pmatrix}\mu_p \\ \mu_n\end{pmatrix} = \begin{pmatrix}2.793 \\ -1.913\end{pmatrix} \text{nm} \qquad 1 \text{ nm} = \frac{e\hbar}{2Mc} = 5.05\times 10^{-24} \text{ erg/G}$$

These are the so-called Schmidt values and form the Schmidt lines. Schmidt (SCH 37) originally proposed attributing μ to the last odd neucleon.

For the case of odd-odd nuclei, if j - j coupling is assumed:

$$\mu = \frac{I}{2}(g_p + g_n) + (g_p - g_n)\,\frac{j_p(j_p+1) - j_n(j_n+1)}{2(I+1)} \text{ nm}, \tag{2.14}$$

where g_p and g_n are the g_s's for the proton and neutron.

Application of (2.11) and (2.13) to a nucleus containing one odd proton yields (BLI 57)

$$Q = Q_j = -\frac{(2j-1)}{2j+2}\left\langle r^2 \right\rangle . \tag{2.15}$$

For one odd neutron

$$Q \approx \frac{Z}{(A-1)^2}\, Q_j .$$

For more than one nucleon in a given subshell

$$Q_{I=j} = Q_J \frac{2j + 1 - 2\lambda}{2j - 1}, \quad \lambda \text{ odd}, \tag{2.16}$$

$$Q_{I=0} = 0 \quad , \quad \lambda \text{ even}, \tag{2.17}$$

where λ is the occupation number of the subshell. The nuclear quadrupole moment Q is negative for a shell less than half filled and positive for a shell more than half filled.

The equation for an odd-odd nucleus is found in reference BLI 57.

2. Collective Model

When the neutron or proton number is far removed from the closed-shell magic number predicted by the shell model, the potential felt by each nucleon no longer appears spherically symmetric. This situation is treated, (BOH 53), (HIL 53), MOT 59), and (NIL 60), by separating nuclear motion into collective and intrinsic modes. A product-type wave function is suggested:

$$\psi = \chi_\Omega \cdot \phi_{vib} \cdot \mathcal{D}_{rot} \tag{2.18}$$

where χ_Ω represents the intrinsic motion of the nucleons, ϕ_{vib} represents the vibrations of the nucleus around its equilibrium shape, and $\mathcal{D}_{rot}$ represents the collective rotational motion of the system as a whole. Enery differences associated with changes in ϕ_{vib} are quite large and, since the work performed concerns the ground state of nuclei, ϕ_{vib} will not be discussed. The quantum numbers associated in describing the collective rotational motion are I, M, and K; i.e., the total angular momentum, its projection on a space axis, and its projection on the intrinsic nuclear axis, respectively. (The rotational spectra of nuclei indicate cylindrical symmetry.)

The particle quantum numbers are obtained by assuming a spherically symmetric harmonic oscillator potential

$$\mathcal{H}_0 = \frac{-\hbar^2}{2M} \nabla^2 + a\, r^2, \tag{2.19}$$

plus a term representing the interaction of the particle and the cylindrically symmetric core,

$$\mathcal{H}_{int} = -b\, \delta\, r^2\, Y_{20} \tag{2.20}$$

(a and b are chosen to correspond to the shell model in the appropriate limit). To both of these is added a spin orbit term and one proportional to $\underset{\sim}{\ell}^2$. The only operator that commutes with the total Hamiltonian is $j_z (= \ell_z + s_z)$, the projection of the particle angular momentum on the axis of deformation ($\mathcal{H}$ is in a coordinate system fixed in the nucleus). It is signified by Ω. Note that parity is also a constant of the motion and that states of $\pm\Omega$ have the same energy.

Now in order to make calculations of magnetic moments, ground-state spins, and other nuclear properties, a representation is chosen with $\mathcal{H}_0$ diagonal. This is $|N, \ell, \Lambda, \Sigma\rangle$ where N is the total oscillator quantum number, ℓ is the eigenvalue of $\underset{\sim}{\ell}^2$, Λ that of ℓ_z, and Σ that of s_z. For states corresponding to a given Ω, the above vectors with $\Lambda + \Sigma = \Omega$ are used as basic vectors. (It should be mentioned that $\mathcal{H}_{int}$ does mix states with $\Delta N = 2$ but energy differences between N and $N \pm 2$ are so large as to render N a fairly good quantum number.) Nilsson (NIL 60) now diagonalizes the total Hamiltonian and computes the energy and eigenfunction corresponding to different values of the deformation δ. For a given nucleus having a certain δ, each Ω level is filled by two nucleons, $\pm\Omega$, and the final ground-state Ω is attributed to the last odd nucleon. The ground state is characterized by $I = \Omega = K$. See Fig. II-3. In the extreme limit of deformation, seen in the rare-earth region, the spin-orbit term is treated as a

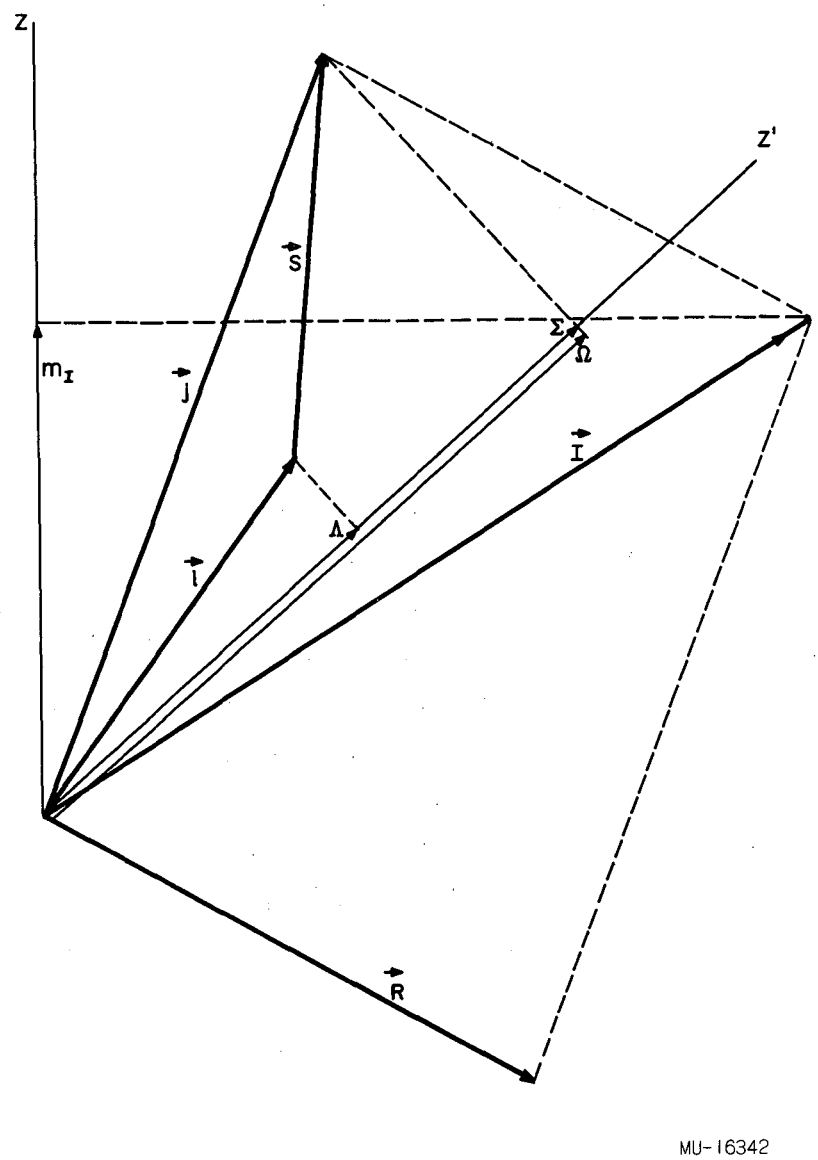

Fig. II-3. Angular-momentum coupling in a collective-model nucleus. In the ground state R is perpendicular to the symmetry axis (Z') and $I = \Omega = K(m_I)$.

perturbation and the quantum numbers become $[N\, n_z\, \Lambda]$, where N is the total oscillator quanta, n_z is the oscillator quantum number along the z' axis, and Λ is as before.

The nuclear moment is

$$\underset{\sim}{\mu} = g_s \underset{\sim}{s} + g_\ell \underset{\sim}{\ell} + g_R \underset{\sim}{R} \quad \text{nm}, \tag{2.21}$$

where $\underset{\sim}{R}$ is the angular momentum of the surface. Since $\underset{\sim}{I}$ is the ground-state spin,

$$\underset{\sim}{\mu} = \frac{\langle \underset{\sim}{\mu} \cdot \underset{\sim}{I} \rangle}{\underset{\sim}{I}^2} \underset{\sim}{I} \quad \text{nm} \tag{2.21a}$$

and

$$\mu = \frac{\langle \underset{\sim}{\mu} \cdot \underset{\sim}{I} \rangle}{I + 1} \quad \text{nm}. \tag{2.21b}$$

For $I \neq 1/2$ this becomes

$$\mu = \frac{I}{I+1}\left[(g_s - g_\ell)\frac{1}{2} \sum_\ell (a^2_{\ell\Omega-1/2} - a^2_{\ell\Omega+1/2}) + g_\ell I + g_R\right]. \tag{2.22}$$

For the case in which $I = 1/2$, a decoupling factor appears and

$$\mu = \frac{1}{I+1}\Bigg[(g_s - g_\ell)\Big[\frac{1}{4}\sum_\ell (a^2_{\ell 0} - a^2_{\ell 1}) + (-)^{I-1/2+\ell}\,\frac{1}{2}\left(I+\frac{1}{2}\right)\sum_\ell a^2_{\ell 0}\Big]$$
$$+ (g_\ell - g_R)\Big[\frac{1}{4} + (-)^{I-1/2}\,\frac{1}{2}\left(I+\frac{1}{2}\right) a\Big] + g_R\, I(I+1)\Bigg], \tag{2.23}$$

where "a" is the decoupling factor. The $a_{\ell\Omega\pm 1/2}$ are the coefficients of the basis vectors ($|N\ell\Lambda\Sigma\rangle$) that describe the last unpaired nucleon, and g_R is the gyromagnetic ratio of all the paired-off protons ($g_R \approx Z/A$).

The decoupling factor "a" can be determined from the rotational spectra. The deformation δ is obtained from the intrinsic quadrupole moment Q_0:

$$Q_0 = 0.8\ Z\ R_z^2\ \delta(1 + \frac{2}{3}\delta), \tag{2.24}$$

$$R_z = 1.2 \times 10^{-13} A^{1/3}\ \text{cm}.$$

The relation between the measured quadrupole moment, Q, and Q_0 is given by

$$Q = \frac{3K^2 - I(I+1)}{(I+1)(2I+3)}\ Q_0 . \tag{2.25}$$

C. Hyperfine Structure

The last term of the total Hamiltonian [Eq. (2.1)] represents that part of the state energy due to the multipole moments of the nucleus interacting with the electric and magnetic fields due to the electrons. The various kinds of interactions are limited by parity arguments and group theoretical considerations (RAM 56). The restrictions are:

(R1) The nucleus may have only odd magnetic moments and even electric moments (parity arguments).
(R2) The largest-order multipole interaction is $(2)^{\ell}$, where $\ell = 2I$ or $2J$, whichever is smaller (group theoretical arguments).

By far the largest contribution to the energy comes from the magnetic dipole of the nucleus in the magnetic field of the electrons. Next is the electric quadrupole moment of the nucleus in the electric field gradient due to the electrons. Octupole and higher-order moments have not been detected with the apparatus currently at this laboratory.

The hyperfine Hamiltonian is then, from (MAR 61),

$$\mathcal{H}_{hfs} = - \underset{\sim}{\mu}_I \cdot \underset{\sim}{H}_N - e^2 \frac{r_N^2}{r_e^3} \sum_k (-)^k C_k^2(\theta_N, \phi_N)\, C_{-k}^2(\theta_e, \phi_e), \tag{2.25}$$

where

μ_I is the nuclear magnetic-dipole moment,

$\underset{\sim}{H}_N$ is the magnetic field at the nucleus due to the electrons,

r_e and r_N are, respectively, the electronic and nuclear radii,

$$C_k^2(\theta_N, \phi_N) = \left(\frac{4\pi}{5}\right)^{1/2} Y_k^2(\theta_N, \phi_N).$$

Before applying an external magnetic field on the atom let us discuss this Hamiltonian.

The nuclear magnetic moment is proportional to its spin:

$$\underset{\sim}{\mu}_I = g_I \mu_0 \underset{\sim}{I} \text{ erg/G}, \tag{2.26}$$

where

μ_0 = Bohr magneton $(= 0.927 \times 10^{-20}$ erg/G),

g_I = nuclear g factor.

For matrix elements diagonal in J, $\underset{\sim}{H}_N$ is proportional to $\underset{\sim}{J}$ and so the first term of $\mathcal{H}_{hfs}$ becomes

$$-\mu_I \cdot H_N = h\, a \underset{\sim}{I} \cdot \underset{\sim}{J} \text{ or } A \underset{\sim}{I} \cdot \underset{\sim}{J}, \tag{2.27}$$

where h is Planck's constant. An evaluation of the proportionality constant yields:

$$h\, a = - \frac{1}{IJ} \mu_I \left\langle H_z \right\rangle_{J,\, m_J = J} \tag{2.28}$$

The magnetic field at the nucleus due to the electrons (only non-s electrons will be considered) is easily found by considering a system of circulating negatively charged particles with permanent magnetic dipole moments. The form resulting for the Hund's rule term (HUB 58) is

$$\langle H_z \rangle_{J,J} = -2\mu_0 \left\langle \frac{1}{r^3} \right\rangle \left(\frac{J(J+1)+L(L+1)-S(S+1)}{2(J+1)} \right.$$

$$+ \frac{2(2L-n^2)}{n^2(2L-1)(2\ell-1)(2\ell+3)} \left\{ \frac{L(L+1)[J(J+1)+S(S+1)-L(L+1)]}{2(J+1)} \right.$$

$$\left. \left. - \frac{3}{4} \frac{[J(J+1)-L(L+1)-S(S+1)][J(J+1)+L(L+1)-S(S+1)]}{(J+1)} \right\} \right). \quad (2.29)$$

Equation (2.29) is for equivalent electrons: $(\ell)^n$ where n is the number of electrons for a shell less than half filled and is the number of holes if the shell is more than half filled. Calculations for more complicated configurations can be found in the literature (MAR 61).

The quadrupole-moment term can be evaluated easily in the $|IJFm_F\rangle$ quantum state (MAR 61):

$$\langle IJFm_F | \text{quadrupole operator} | IJFm_F \rangle = \frac{-e^2 q_J \, Q}{2IJ(2I-1)(2J-1)} \left[\frac{3}{4} K(K-1) - \right.$$

$$\left. - I(I+1)J(J+1) \right], \quad (2.30$$

where

$K = I(I+1) + J(J+1) - F(F+1)$,

$q_J = \langle J, m_J = J | \sum_i \left\langle \frac{1}{r^3} \right\rangle_i (3\cos^2\theta_i - 1) | J, m_J = J \rangle$ (sum over electrons),

$Q = \langle I, m_I = I | \sum_k r_k^2 (3\cos^2\theta_k - 1) | I, m_I = I \rangle$ (sum over protons).

The quantity $-e^2 q_J \, Q$ is called the electric-quadrupole coupling constant, and is written hb or B.

The electric-quadrupole field (q_J) can be evaluated fairly easily for the case of equivalent electrons coupling to the Hund's rule ground state (MAR 61):

$$q_J = \mp \left\langle \frac{1}{r^3} \right\rangle \left[\frac{3K'(K'-1) - 4L(L+1)J(J+1)}{(2L-1)(J+1)(2J+3)} \right] \left[\frac{2\ell - n^2}{n(2\ell-1)(2\ell+3)} \right] , \tag{2.31}$$

where $K' = J(J+1) + L(L+1) - S(S+1)$.

For less than a half-filled shell, n is the number of electrons and the minus sign is used; for more than a half-filled shell, n is the number of holes and the positive sign is used.

Nuclear model theories have yet to satisfactorily predict Q; in fact, its enormity in the rare-earth region led to the collective-model nucleus.

Because both $\langle H_z \rangle$ and q_J contain the term $\langle 1/r^3 \rangle$, the nuclear magnetic moment and quadrupole moment cannot be extracted from a or b without good electronic wave function. If, however, μ_I and "a" have been determined independently for another isotope of the same element, we can use the so-called Fermi-Segrè relation (good to about 1%):

$$\left(\frac{a}{g_I} \right)_1 = \left(\frac{a}{g_I} \right)_2 , \tag{2.32}$$

where the subscript 1 refers to the known values and 2 to the unknown μ_I.

Essentially $\langle 1/r^3 \rangle$ has been measured for isotope 1, and corrections to this term plus other effects due to the different nucleus cause the relation to be good to about 1%. The proposed $\langle 1/r^3 \rangle$ values of Judd and Lindgren (JUD 61)are also used to determine μ_I in this work.

A simplified form of the hyperfine Hamiltonian is

$$\mathcal{H}_{hfs} = ha\, \underset{\sim}{I} \cdot \underset{\sim}{J} + \frac{hb}{2IJ(2I-1)(2J-1)} \left[\frac{3}{4} K(K-1) - 4I(I+1)J(J+1) \right] , \tag{2.33}$$

where $K = I(I+1) + J(J+1) - F(F+1)$.

We now have an atom sitting in a state which can be described with the quantum numbers I, J, F having a degeneracy of (2F + 1).

Application of an external magnetic field (H) removes this degeneracy; the hfs Hamiltonian becomes

$$\mathcal{H}'_{hfs} = \mathcal{H}_{hfs} - g_J \mu_0 \underset{\sim}{J} \cdot H - g_I \mu_0 \underset{\sim}{I} \cdot H. \qquad (2.34)$$

The last two terms represent the magnetic field interacting with the electrons acting as a whole and interacting with the nucleus. As long as the magnetic field remains below hundreds of thousands of gauss the electrons will act as a unit. At low values of H(0 to 15G), I, J, F, m_F remain fairly good quantum numbers; while as H increases, F and m_F lose meaning and I, m_I, J, m_J describe the system. Energy-level differences are measured as a function of H, and a fit to these values is made by choosing proper a, b, I, J, g_I, and g_J values. Again the data are usually accurate enough to determine a and b reasonably well; sometimes the value of g_J is improved, but g_I is a small effect and is for the most part computed from "a".

III. EXPERIMENTAL TECHNIQUE

How does one measure I, J, a, and b with the atomic-beam technique? The beam method provides a means of placing atoms in a free state, so following the remarks made in Sec. II-C, each atom exists in an I, J, F state having (2F + 1) degeneracy. The temperature of the beam mixes many of the J states; i.e., atoms in the beam exist in all the low-lying J states. The nucleus usually rests in its ground-state spin, and all the F levels (which are separated by radiofrequency energies only) corresponding to I, J, are occupied. See Fig. III-1.

Upon application of a magnetic field, the degeneracy at each F level disappears, and one has the situation in Fig. III-2, and the following Hamiltonian:

$$\mathcal{H}_{hfs} = h\, a\, \underset{\sim}{I} \cdot \underset{\sim}{J} + h b f(\underset{\sim}{I}\, \underset{\sim}{J}) - g_J \mu_0 \underset{\sim}{J} \cdot H - g_I \mu_0 \underset{\sim}{I} \cdot H. \tag{3.1}$$

Now

$$g_I \approx \frac{1}{2000}\, g_J ,$$

so the energy-level differences within the same F are determined mostly by $g_J \mu_0 \underset{\sim}{J} \cdot H$. Since the representation for low values of H is $|I\ J\ F\ m_F\rangle$,

$$g_J\, \mu_0 \underset{\sim}{J} + g_I \mu_0 \underset{\sim}{I} = g_F\, \mu_0 \underset{\sim}{F} \tag{3.2a}$$

where

$$g_F \approx g_J\, \frac{F(F+1) + J(J+1) - I(I+1)}{2F(F+1)} . \tag{3.2b}$$

Thus, from a knowledge of g_J and either J or I–(these are usually available from optical data, paramagnetic experiments, or other beam work)–coupled with measurements of ΔE, the remaining unknown (I or J) can be found.

As the magnetic field is increased, deviations from these Zeeman levels occur because $-g_J \mu_0 \underset{\sim}{J} \cdot H$ has nonzero matrix elements between states of different F, and its energy contribution becomes

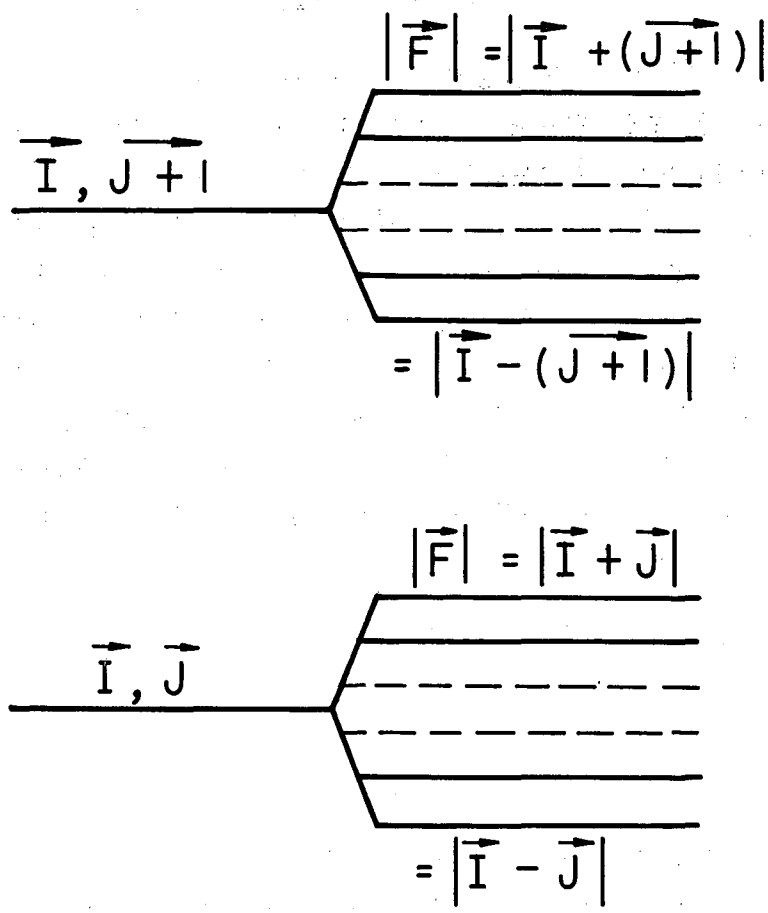

MU-28996

Fig. III-1. The coupling of I and J to various F states.

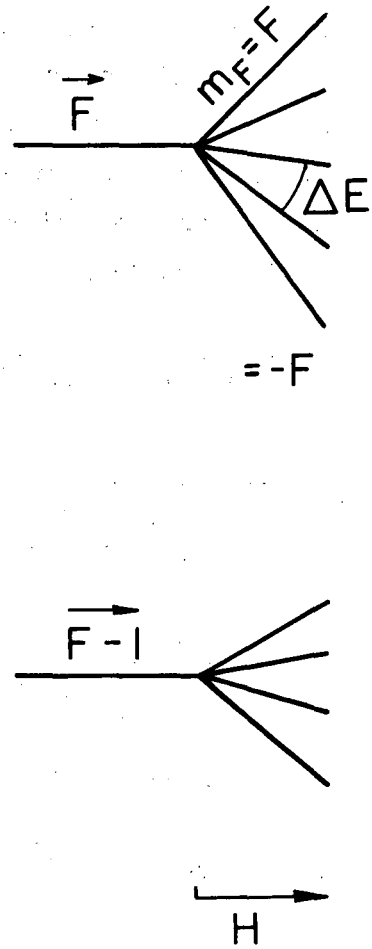

MU-28997

Fig. III-2. Breakdown of (2F+1)-fold degeneracy upon application of a magnetic field.

close to the order of these ΔF energies. The determination of a and b is made by finding energy-level differences as a function of H for different F values. These data are analyzed by a 7090 program which diagonalizes $\mathcal{H}'_{hfs}$ at the appropriate field values and chooses the best value of a and b consistent with ΔE.

Optimum a and b values are found by minimizing a χ^2 function defined in the following way:

$$\chi^2 = \sum_i [f^i_{obs} - f^i_{theo}(a, b, g_J, g_I)]\, w_i ,$$

where

$$w_i = \frac{1}{(\Delta f^i_{obs})^2 + (\frac{\partial f^i_{theo}}{\partial H^*} \Delta H^{*i})^2},$$

$$H^* = \frac{(-g_J + g_I)}{h} \mu_0 H,$$

f^i_{obs} = experimental frequency,

Δf^i_{obs} = uncertainty in the experimental frequency,

H = magnetic field in C region,

f^i_{theo} = theoretically expected resonance frequency for a given a, b, g_J, g_I.

If χ^2 converges to N - x, where N is the number of observables and x the number of independent variables, then the uncertainties in a and b approximately correspond to a standard deviation. If χ^2 is less than N - x, the uncertainties quoted are larger than a standard deviation, and vice versa. The program can also find the best value of g_J and g_I (if the data are accurate enough) to satisfy the information given.

A brief description of the program is available in references (PET 60) and (MAR 61).

In order to measure energy-level differences to find a, b, I, J, an atomic-beam machine was utilized. A schematic diagram of such a machine appears in Fig. III-3. It consists essentially of a beam source, a magnet system, a detector, and appropriate rf equipment to induce transitions between energy levels. A vacuum system, beam-collimating slits, and various electronic power supplies are also required.

The beam source consists of a chamber in which the material to be studied can be heated. The substance is placed in an oven (Fig. III-4) and heated—by electron bombardment in this case. The oven itself has a small slit through which the vaporizing material escapes down the machine.

The magnet system consists of two inhomogeneous magnets, A and B, and a homogeneous one, C. An atom coming out of the oven first sees the A magnet, then the C, then the B magnet. The A and B magnets are designed to produce a large H field as well as a field gradient at the beam site. The atoms in the beam take on definite m states (and therefore a definite μ) in the A magnet, are deflected due to $\partial H/\partial Z$, and enter the C region in the same m state--provided H does not change so rapidly that the atom cannot follow it adiabatically. In the C field an rf loop is provided so as to induce transitions between different m states (Fig. III-5). The atom then enters the B field, whose gradient is set so that unless the effective μ of the atom just changes sign, the atom is deflected farther from the center line and does not reach the detector. In the high fields existing ($\approx$ 10 000 G) in A, B region, the magnetic moment of an atom is mostly due to $g_J \mu_0 m_J$,† and so m_J must change sign (+ 1/2 to - 1/2 in the case of J a half integer and +1 to -1, a multiple quantum transition, in the case of integer J). If the rf frequency is at a suitable resonance then the B magnet will cause the atom to swing back to the neutral axis, negating the effect of A. This is called the flop-in technique (ZAC 42).

---

† $\mu = -\partial W/\partial H$; $W = h a m_I m_J + hb\, f(FIJ) - g_J \mu_0 m_J H - g_I \mu_0 m_I H$.

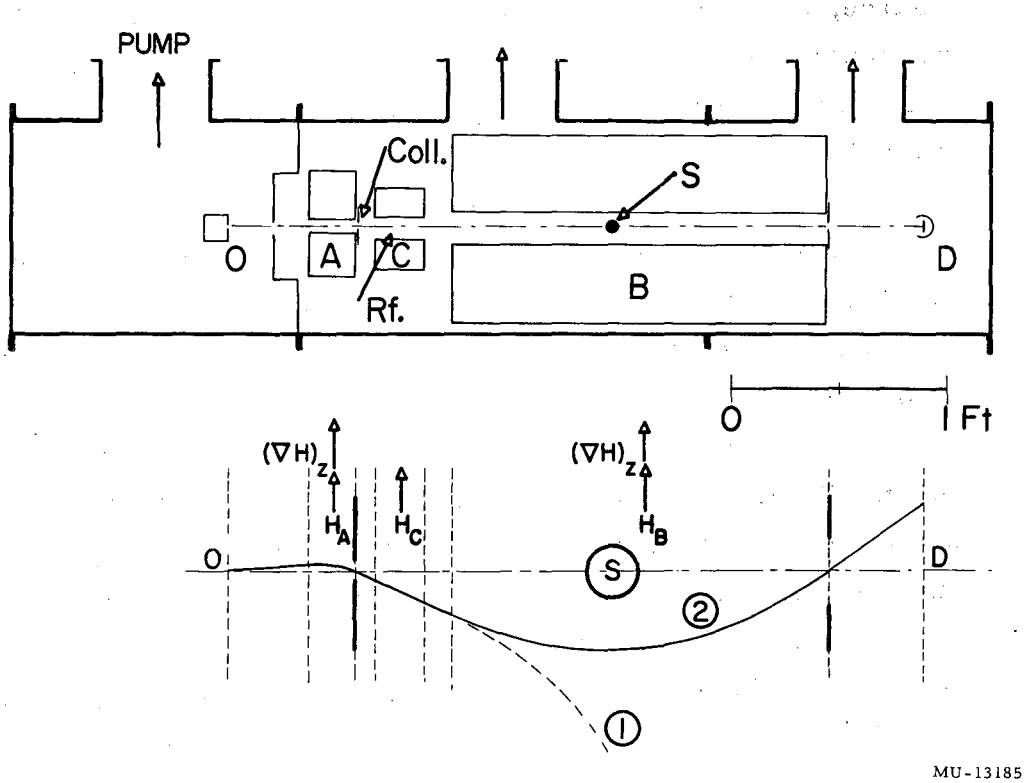

Fig. III-3. Schematic diagram of an atomic-beam machine.

O = Oven
A, B = Deflecting magnets
C = Homogeneous magnet where transitions are induced
S = Stop wire
D = Detector.

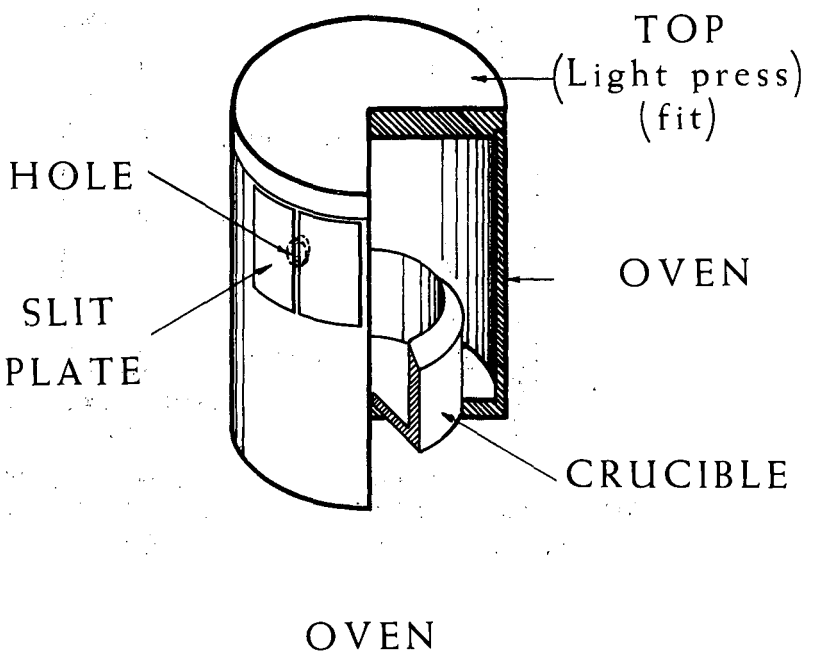

MU-13888

Fig. III-4. Tantalum oven used to contain radioactive isotopes.

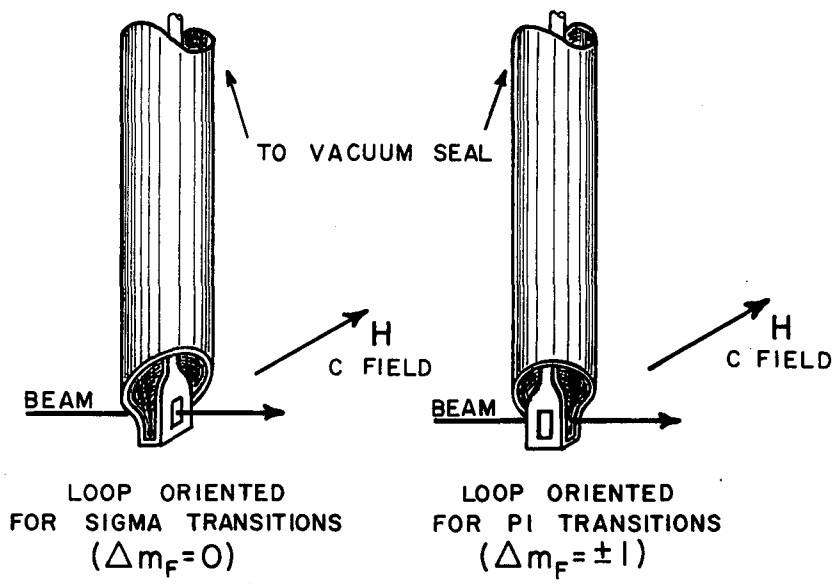

MU-18042

Fig. III-5. Radiofrequency loop to induce transitions. (Selection rules are indicated.)

In order to calibrate the C field, resonances in stable K^{39} were found. The hfs and nuclear moment are well known (RAM 56) and so a resonance at a given frequency corresponds to a certain magnetic field in the C magnet. The frequency is usually set and the C field varied until a resonance appears. The K^{39} oven source is kept in the "buffer" chamber and whenever a field calibration or check is desired, the oven is placed along the beam axis.

The type of detector used varies with the substance. One can detect K^{39} by using a hot wire; i.e., a wire through which current is passed and whose work function is less than the ionization potential of K^{39}. A K^{39} atom hits the wire, one electron is removed from the atom, and, because of the work function-ionization potential condition, the ion comes off onto a positively charged plate. A dc beam current is measured which increases at a resonance. The radioactive materials do not have suitable ionization potentials and they are detected by using flamed-platinum buttons (Fig. III-6). The atoms stick to the platinum and the beta activity is measured by using a continious-flow beta counter with methane gas (Fig. III-7). A resonance is found by setting the C field by with K^{39} and then varying the rf frequency at this static field until the beta activity of the foils indicate a resonance line has been found.

In the experiments performed, two beam machines were used: Machine A (ALP 61) and (WHI 62), and Machine B (BRI 57) and (CAB 60). The details of the running technique involved taking 5- to 9-min resonance exposures with fixed C field and fixed frequency intermixed with direct beams (stop-wire S removed) of 1-min intervals for normalization purposes. Sometimes, due to unusual chemical effects, resonance buttons taken at different times during the run were used to normalize the data, i.e., Tb^{161}.

The radioactive isotopes were produced by neutron bombardment of the stable metal for a time interval suited to the isotope of interest. Figure III-8 shows the quartz-encapsulated metal together with an Al holder. Irradiations were done either at the Vallecitos General Electric Test Reactor in Pleasanton, California or at the

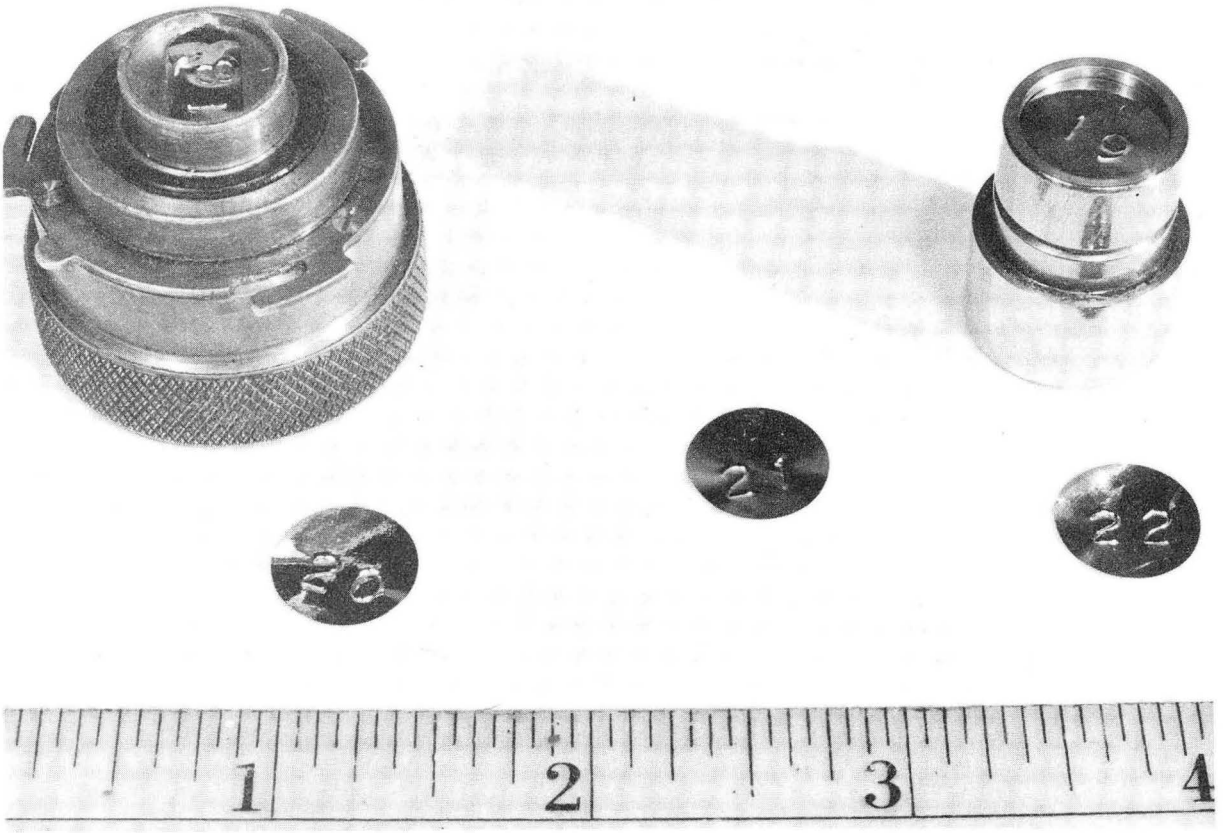

ZN-2936

Fig. III-6. Platinum foils (0.001 in.) shown with machine button holder and beta-counter holder.

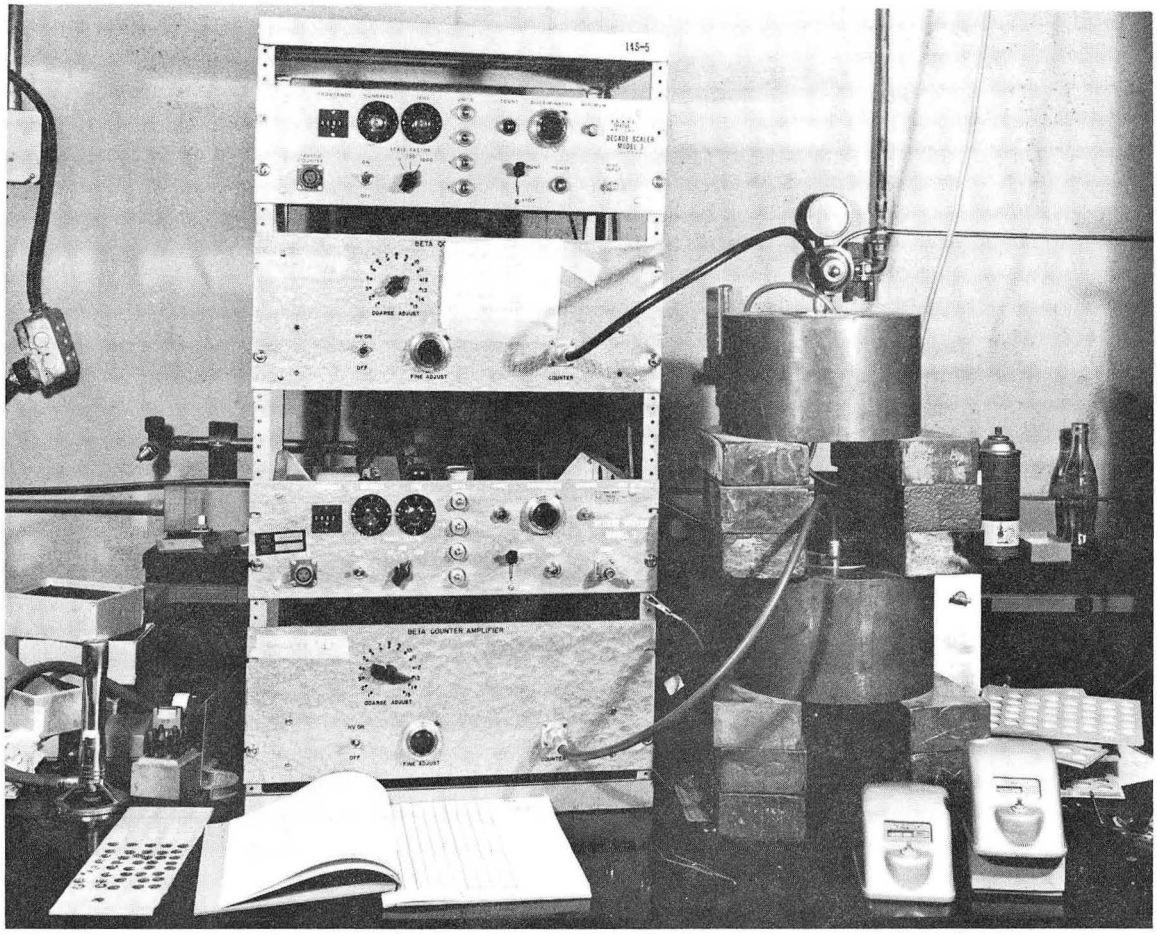

ZN-3712

Fig. III-7. Beta counters and associated electronics.

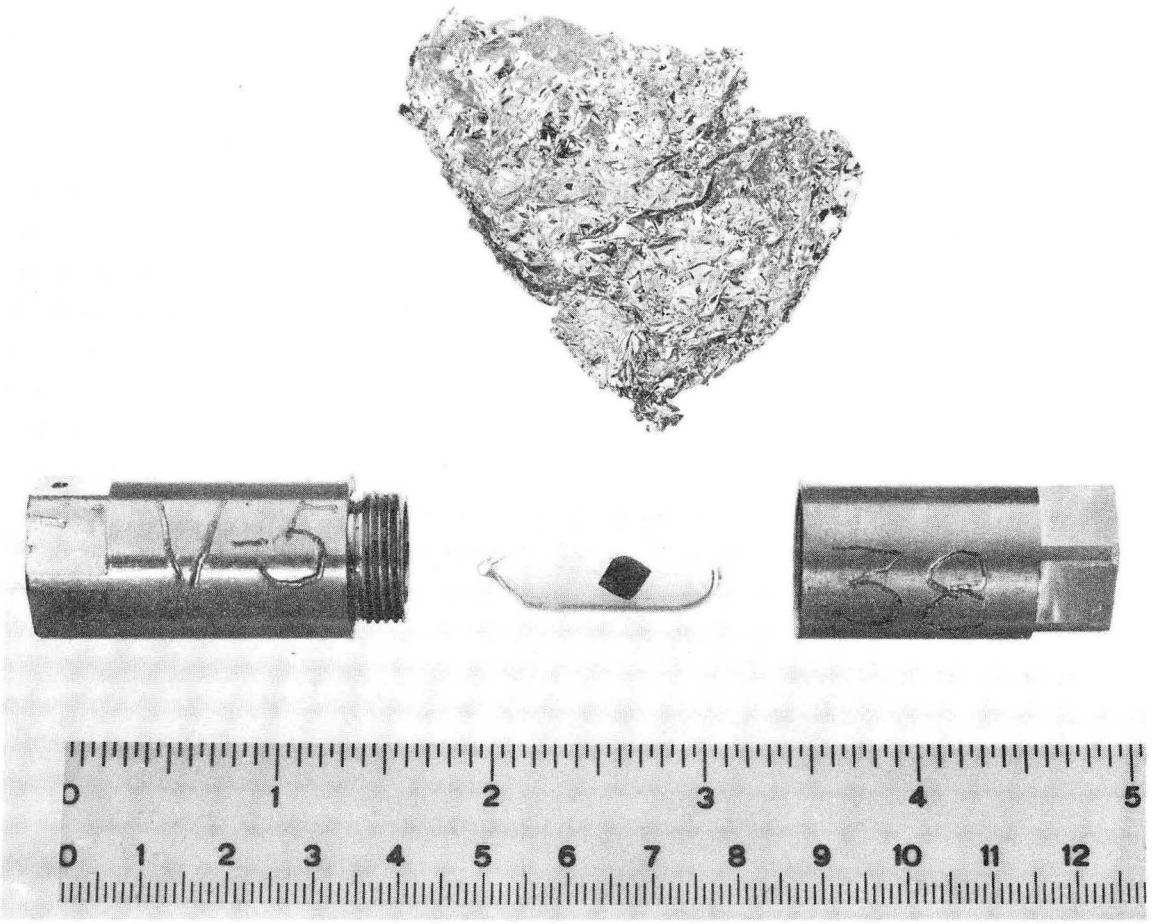

ZN-3714

Fig. III-8. Erbium metal ready for irradiation at Valecitos. The quartz capsule is wrapped in Al foil (top) to promote heat conduction before being enclosed in Al capsule.

Materials Testing Reactor in Arco, Idaho. The maximum flux available at Vallecitos is 1×10^{14} n/cm^2-sec for bombardments of hours to days, and 2×10^{14} n/cm^2-sec at Arco for bombardments up to 10 days, while 5×10^{14} n/cm^2-sec is available in the core for a 3-week cycle.

Figure III-9 shows Machine A as of October 1962; Fig. III-10 shows Machine B. The oven loader for Machine B is shown in Fig. III-11. The lead cave shown on B was necessary to allow the experimenter to minimize his radioactive dosage.

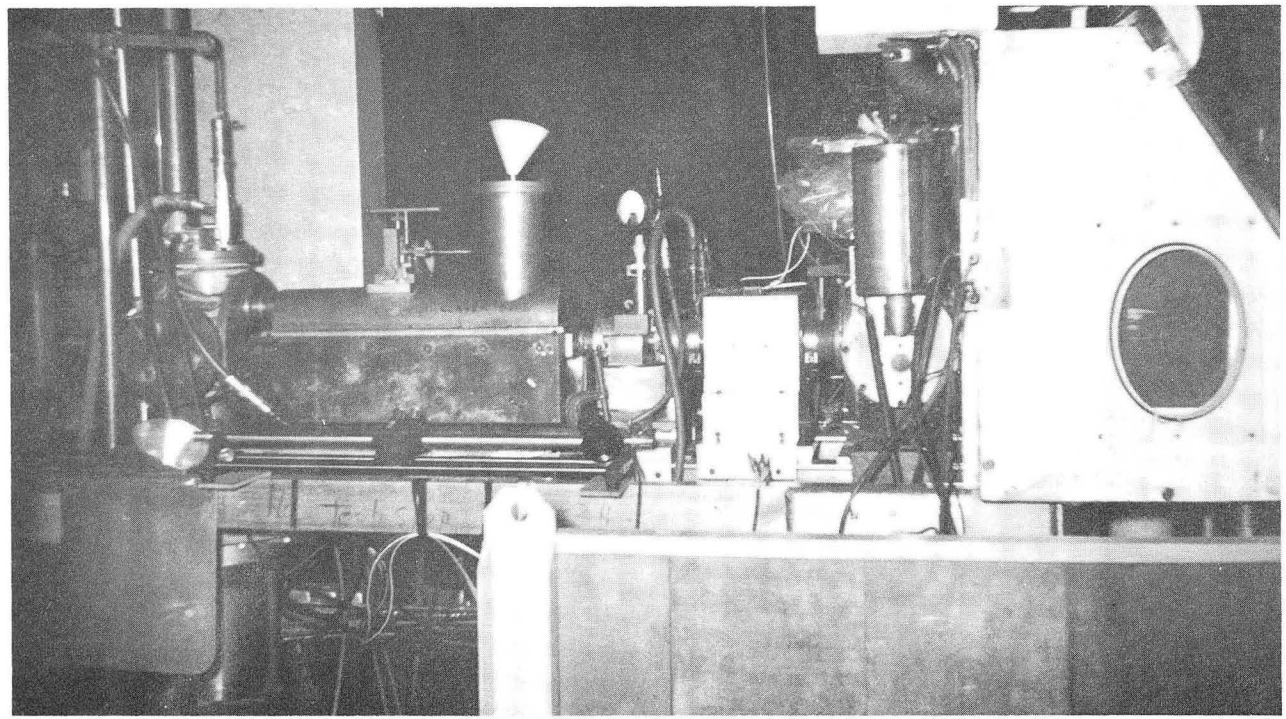

ZN-2213

Fig. III-9. Atomic-beam Machine A.

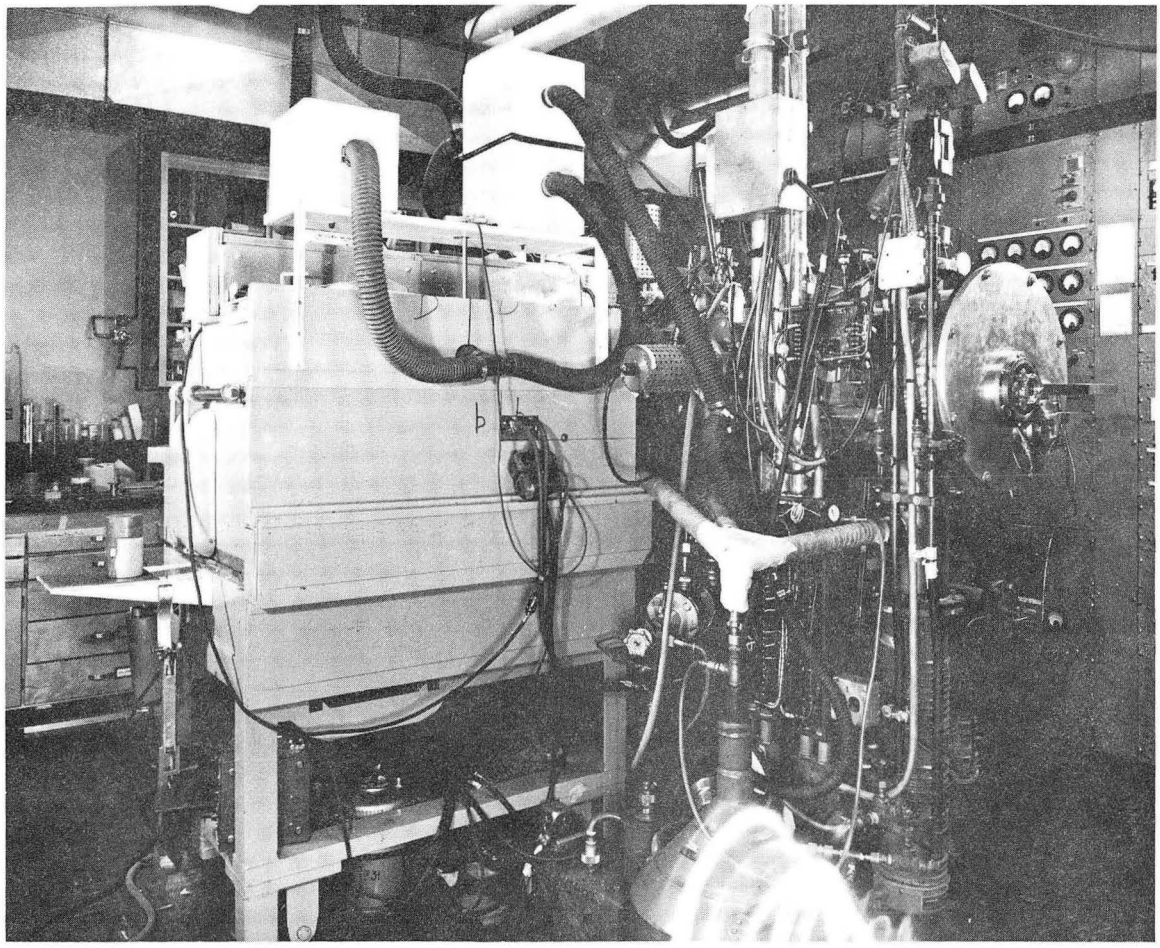

ZN-3715

Fig. III-10. Atomic-beam Machine B.

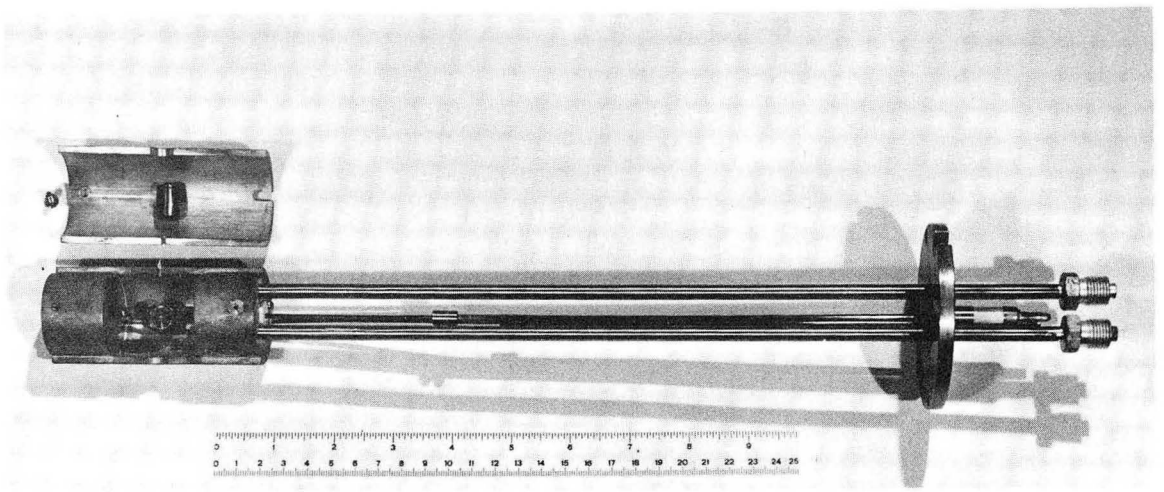

ZN-3713

Fig. III-11. Oven loader for atomic-beam Machine B together with Ta oven.

IV. EXPERIMENTAL RESULTS

A. Thulium-171

1. Introduction

Ketelle and Boyd (KET 48) first identified Tm^{171} and reported that it decayed by the emission of 0.100-MeV electrons with a half-life of 680 days. Further study of its beta decay, (SMI 57) and (SHA 61), indicated the level scheme shown in Fig. IV-1. The ground-state electronic structure was determined by optical spectroscopy (MEG 42) and is $(4f)^{13}(6s)^2$, $^2F_{7/2}$. The g_J was accurately determined from the hfs determination of Tm^{170} (CAB 60). The value differs from the pure Russel-Saunders case but is easily obtained once relativistic and diamagnetic corrections are applied as discussed in the above reference. It is essentially a one-electron problem.

The spin of Tm^{171} was found to be 1/2 (CAB 60), yielding the hfs diagram shown in Fig. IV-2.

2. Experiment

Several chunks of 99.9%-pure erbium metal (each piece ≈ 300 mg) were encapsulated and sent to Arco for a 3-week irradiation at 5×10^{14} n/cm^2-sec. Each piece was wrapped in Al foil to prevent fusing with others. The reaction producing Tm^{171} was

$$Er^{170}(n,\gamma)\,Er^{171} \xrightarrow[\beta^-]{7.5\,h} Tm^{171}\,(1.9\text{ yr}).$$

A few months were allowed to elapse before running, to allow the 9-day Er^{169} to decay.

Very few problems arose in getting a stable usable beam; the material came off at relatively low power. To identify the isotope a button was exposed to the full beam for a long time, and a γ spectra was obtained by using a 200-channel Penco analyzer with a ThI crystal. The result was interesting; it is discussed in Subsec. IV-A-4.

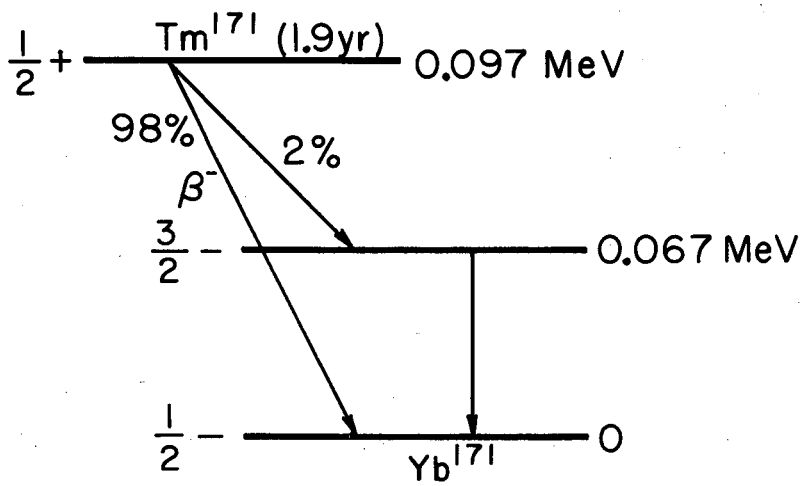

MU-28993

Fig. IV-1. Decay scheme for Tm^{171}.

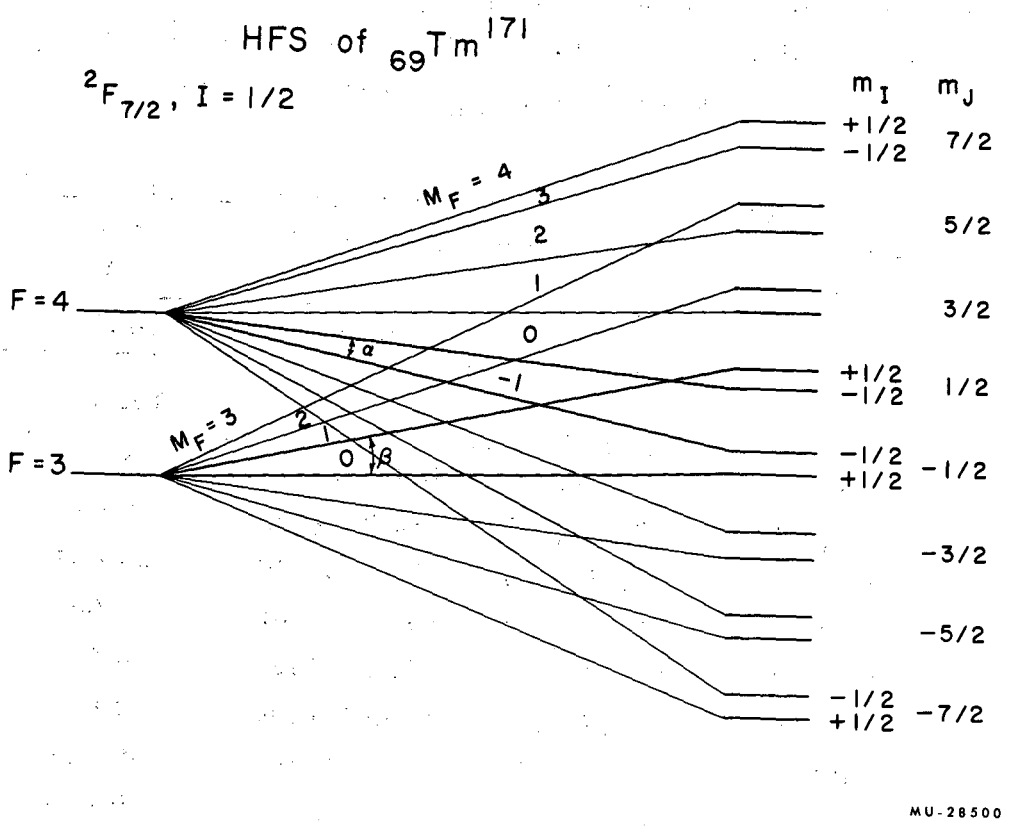

Fig. IV-2. Hyperfine structure of Tm^{171} (schematic).

3. Results

Nine resonances were found and served to give reasonably good values of a, g_J, and g_I. As seen in Table IV-1, five β and four α transitions in fields ranging from 79 to 217 G constituted the data. An α transition as seen in Fig. IV-2, is one involving F_{max} and $\Delta F = 0$, while a β involves $(F_{max}-1)$ and $\Delta F = 0$.

Table IV-1. Thulium-171 resonances and χ^2 fit.[a]

a(Mc)	g_J	Δa	Δg_J	χ^2
372.0710	- 1.141155	5.9403	0.000097	1.25

ν_K(Mc)	H(G)	ν_{exp}(Mc)	Residual	Transition
139.980(40)	117.672(23)	164.950(50)	-0.039	α
160.000(50)	128.875(27)	180.750(50)	-0.019	α
310.000(80)	200.654(35)	282.230(100)	-0.051	α
350.000(100)	217.808(42)	306.700(50)	0.049	α
80.030(50)	79.154(37)	142.360(50)	0.011	β
120.140(100)	105.890(61)	190.450(100)	0.003	β
140.000(40)	117.684(23)	211.650(50)	-0.011	β
209.950(50)	154.646(25)	278.125(50)	0.009	β
310.000(80)	200.654(35)	360.750(50)	0.020	β

Residual = $\nu_{exp} - \nu_{theo}$

Transitions: α $F = 4$; $m_F = 0 \leftrightarrow -1$

β $F = 3$; $m_F = 1 \leftrightarrow 0$.

[a]Data taken on Machine B.

The results of these measurements are:

$$a = \pm 372.1(5.9)\ \text{Mc}, \qquad (4.1)$$
$$g_J = -1.14116(10).$$

Using published data (RIT 62) on Tm^{169} which include

$$a = -374.1374(16)\ \text{Mc},$$
$$g_J = -1.14119(4),$$
$$\mu_I(\text{uncorr}) = -0.227(3)\ \text{nm}, \qquad (4.2)$$
$$\mu_I(\text{corr}) = -0.229(3)\ \text{nm},$$

the nuclear moment of Tm^{171} becomes

$$\mu_I(\text{uncorr}) = \pm 0.225(5)\text{nm}, \qquad (4.3)$$
$$\mu_I(\text{corr}) = \pm 0.227(5)\ \text{nm}.$$

The Fermi-Segrè relation was used to obtain the above values.

With the suggested value of $\langle 1/r^3 \rangle$ of Judd and Lindgren (JUD 61) and Eqs. (2.28) and (2.29) we calculate

$$\mu_I\left(\left\langle \frac{1}{r^3} \right\rangle\right) = \mu_I(\text{corr}) = \pm 0.242(15)\ \text{nm}. \qquad (4.4)$$

Since Eq. (4.4) was obtained by using $\langle 1/r^3 \rangle$ and a, no diamagnetic correction is necessary. The reliability of Judd and Lindgren's wave functions is indicated by the fact that Eq. (4.4) and μ_I(corr) overlap.

4. Interpretation

Since thulium is well into the rare-earth region, the moment will only be compared with the collective model. Thulium-171, asymptotic state [411] 1/2+, has spin 1/2, so knowledge of the decoupling factor is required as well as the deformation, δ. The rotational spectra of Tm^{171} yields a = - 0.86. The nucleus has no quadrupole interaction with the electrons so only an estimate of δ is possible. It is probably very close to 0.29, the value of δ for Tm^{169} (MOT 59).

Now by using Eq. (2.23) and obtaining the $a_{\ell 0}$ and $a_{\ell 1}$ values from Table 1b of (NIL 60),

$$\mu = -0.300 \text{ nm}, \qquad \delta \approx 0.3, \tag{4.5}$$
$$\mu = -0.132 \text{ nm}, \qquad \delta \approx 0.2.$$

The measured value being $\pm 0.227(5)$ indicates surprisingly good agreement with the model, considering approximations in g_R and δ.

Figure IV-3 indicates the gamma spectra taken on Tm^{171}. The 22.5-keV peak represents the iodine escape peak of the K x-rays of Yb^{171}; i.e., the 67-keV level is highly converted, giving $\approx$ 53-keV x-rays (67 keV minus the binding energy of K electrons of Yb^{171}). These $\approx$53 keV x-rays sometimes knock out the K electrons of I in the ThI crystal, yielding electrons with energy $\approx$ 25 keV and x-rays of iodine with 28 keV. The K x-rays of iodine are not detected (escape), while the energy of the $\approx$25-keV electrons is recorded. Thus, within the limits of the experiment, we see that the 22.5-keV peak corresponds to the recording of the $\approx$25 keV electrons. The $\approx$ 84-keV peak is strange and may either represent a contaminant of the 99.9-% pure Er or a real rotational level of Tm^{171} unreported by other researchers.

Figures IV-4 and IV-5 are typical resonances obtained on Machine B.

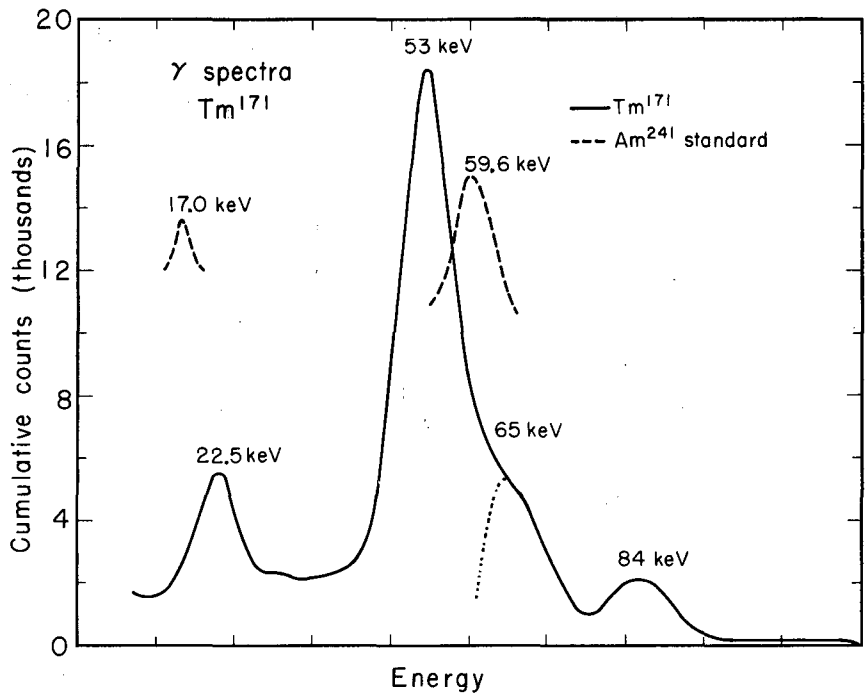

Fig. IV-3. Gamma spectra of Tm^{171} produced from $Er^{170}(n, \gamma)\ Er^{171} \xrightarrow[\beta^-]{7.5\,h} Tm^{171}$.

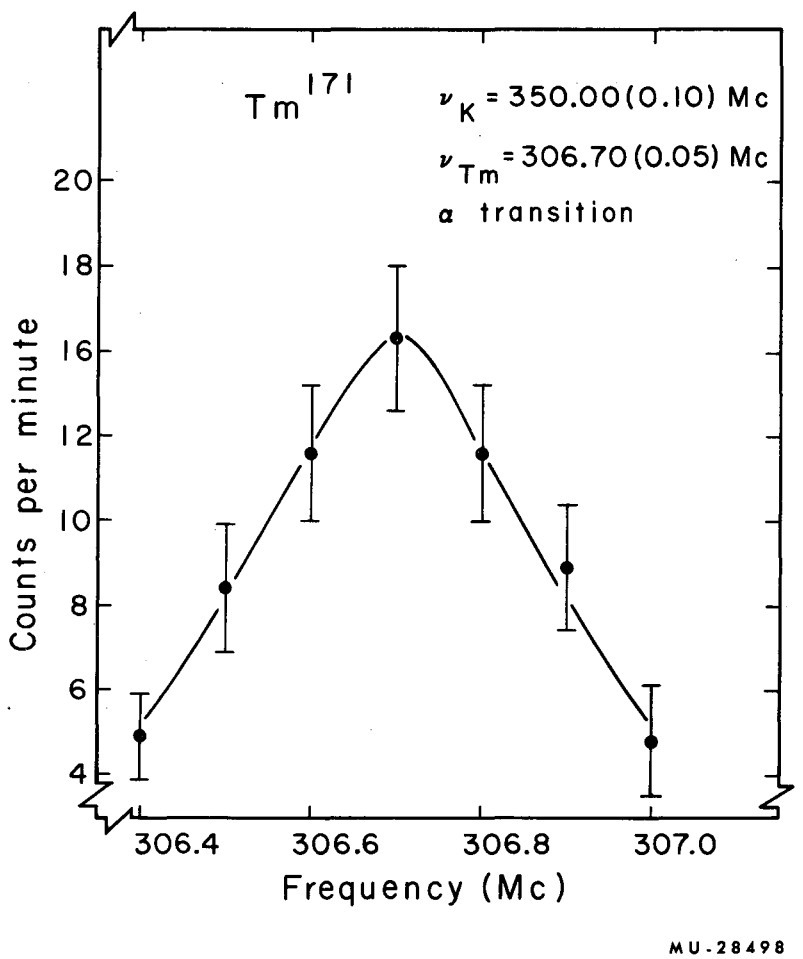

Fig. IV-4. Alpha transition at ν_K = 350.000 Mc (H = 217.808 G, F = 4, $m_F = 0 \leftrightarrow -1$).

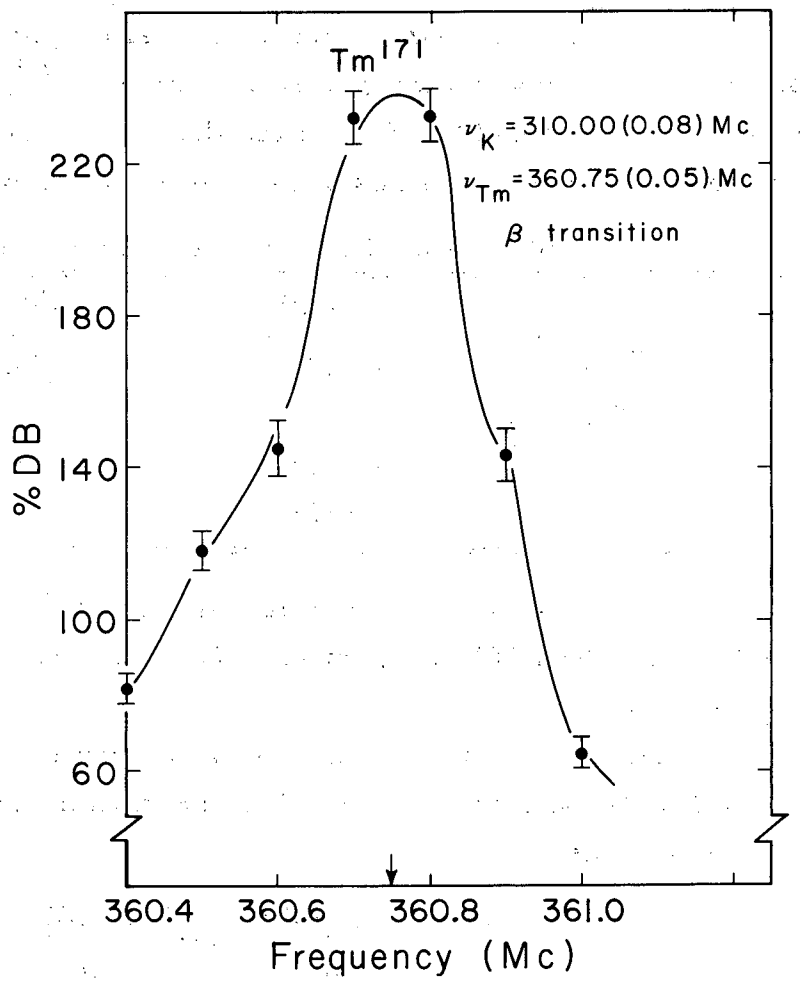

MU-28499

Fig. IV-5. Beta transition at ν_K = 310.000 Mc (H = 200.654 G, F = 3, m_F = 1 ↔ 0).

B. Terbium-161

1. Introduction

The atomic-beam group at Heidelberg have determined four J states with corresponding g_J's from stable Tb^{159}(PEN 60). A study has been made (CAB 60) to determine the configurations that may produce these numbers. The result is reproduced in part in Table IV-2.

Table IV-2. Terbium electronic structure.

J	g_J(exp)	Configuration
15/2	-1.3225	$(4f)^9$
15/2	-1.4563	$(4f)^8(5d)$
13/2	-1.4633	$(4f)^8(5d)$
11/2	-1.5165	$(4f)^8(5d)$

The decay scheme and half-life of Tb^{161} were measured by (HAN 58) and (SMI 56), respectively (τ = 6.8 days).

2. Experiment

The isotope was produced by neutron bombardment on stable Gd metal at Arco, Idaho. The irradiation time was ten days; Tb^{161} evolved as follows:

$$_{64}Gd^{160}(n,\gamma)\,Gd^{161} \xrightarrow[\beta^-]{3.7\ \text{min}} {}_{65}Tb^{161} \xrightarrow[\beta^-]{6.8\text{d}} {}_{66}Dy^{161}.$$

A low-capture cross section (0.8b) as well as just 20% abundance of Gd^{160} caused a marginal, though reasonable, experiment. The only other active contaminant was Gd^{159}(τ = 18 h) which decayed during the 2 to 3 days that elapsed while the sample was being transported from Idaho.

3. Results

By using the above mentioned J and g_J values and the technique discussed in Sec. III, a spin search was performed at ν_K = 4.0 Mc(H = 5.566 G) and ν_K= 8.0 Mc(H=10.865 G). As shown in Figs. IV-6 and IV-7 only the J = 11/2 and 13/2 were clearly seen.

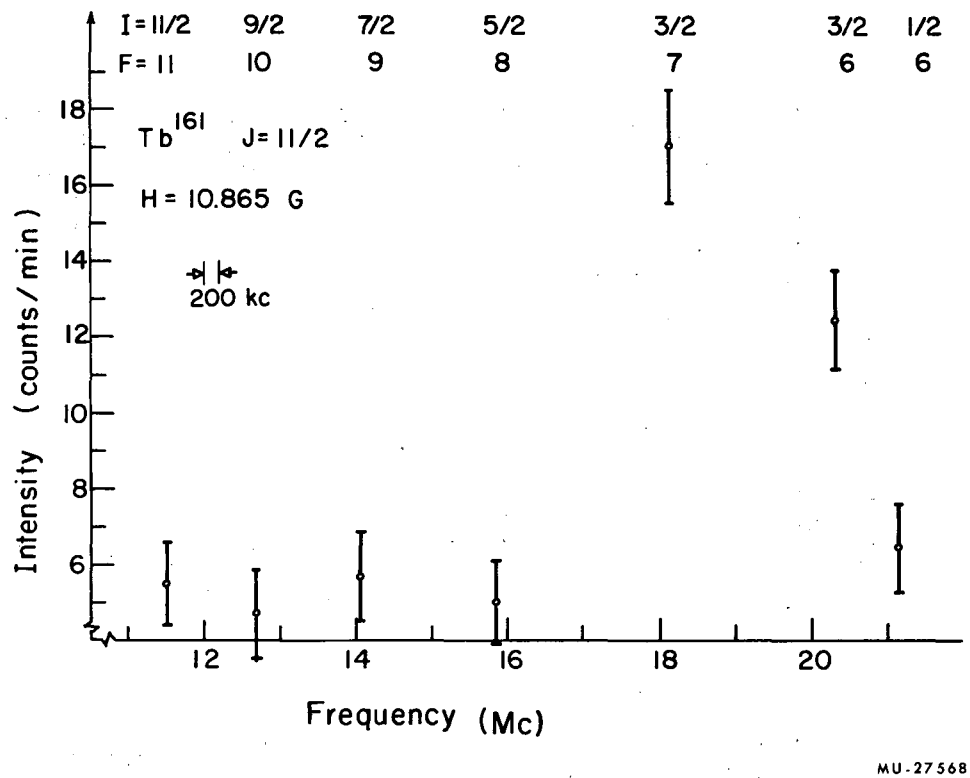

Fig. IV-6. Spin search for Tb^{161} at ν_K = 8.0 Mc (H = 10.865 G, J = 11/2).

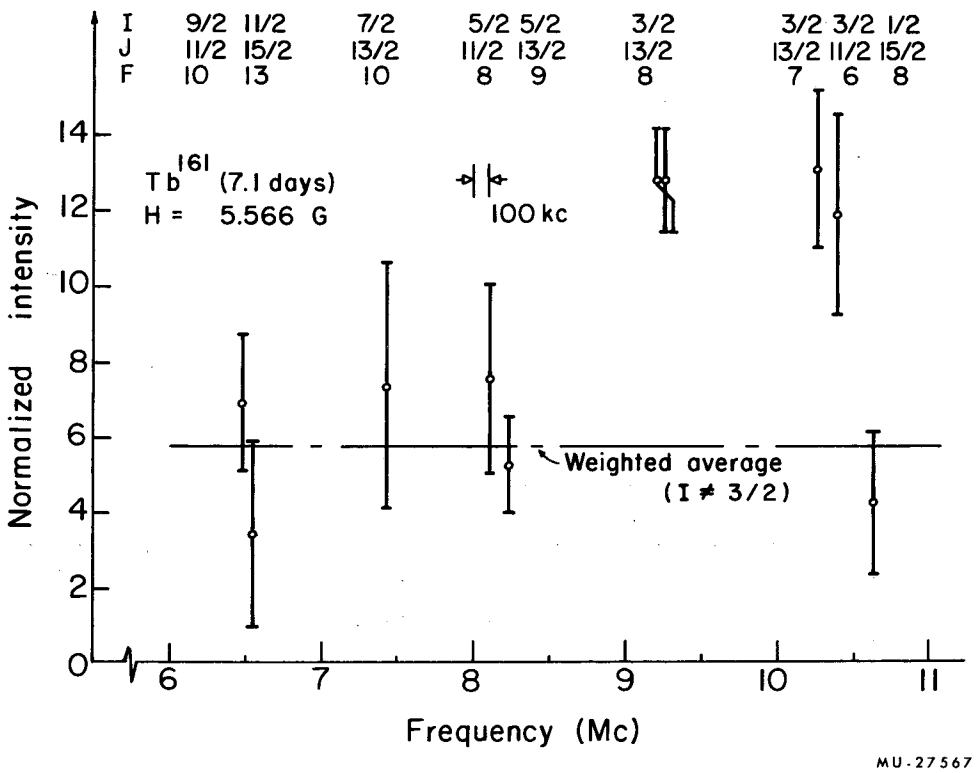

Fig. IV-7. Spin search for Tb^{161} at ν_K = 4.0 Mc (H = 5.566 G).

(Two high points belonging to $J = 15/2$ were observed but with poor statistics.) The results indicate $I = 3/2$. Figure IV-8 shows a schematic hfs diagram together with the actual α and β transition observed. Figure IV-9 is a plot of a resonance button over time; it indicates $\tau = 6.9 \pm 0.8$ days.

4. Interpretation

The measured spin, 3/2, of Tb^{161} agrees very well with the collective-model state assignment [411] 3/2 assumed by (MOT 59) to explain the decay schemes of $A = 161$ isotopes.

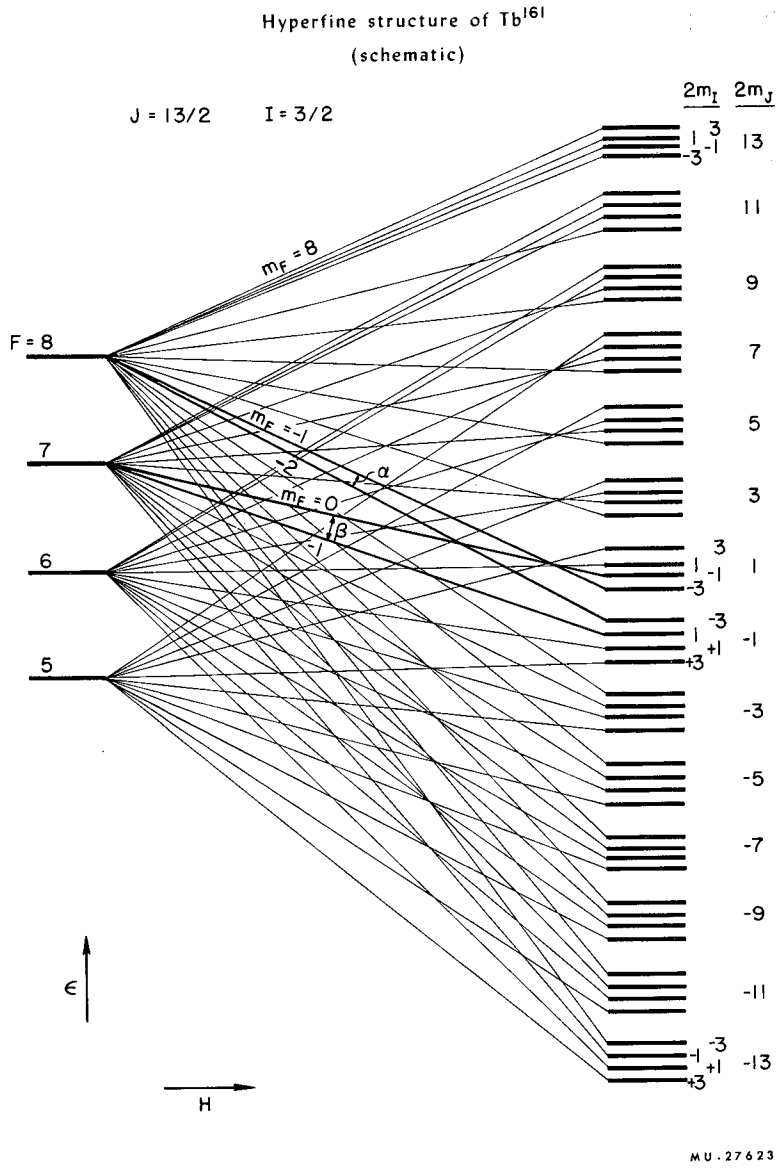

Fig. IV-8. Hyperfine structure diagram for Tb^{161} [J = 13/2; $(4f)^8 5d(6s)^2$] showing α and β transitions.

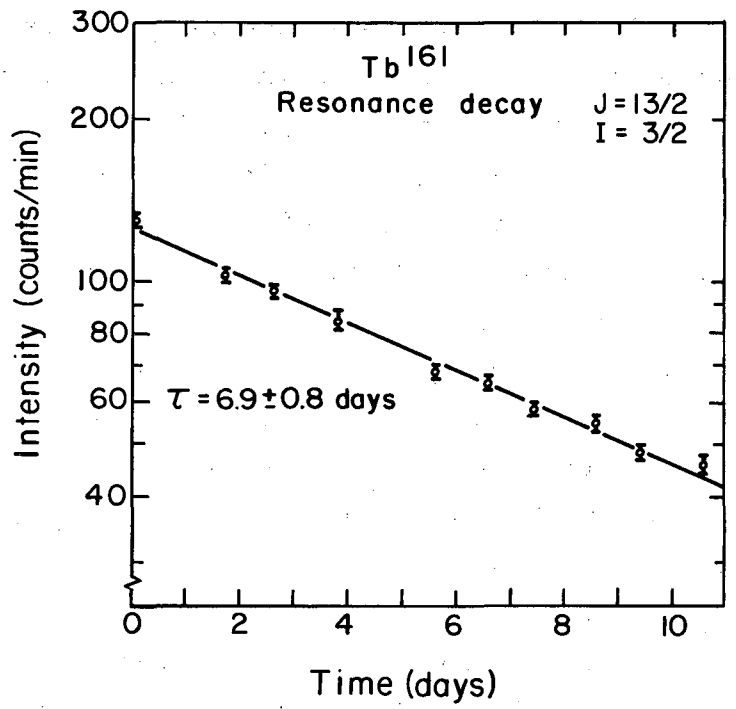

Fig. IV-9. Decay of a resonance button of Tb^{161} ($I = 3/2$, $J = 13/2$).

C. Erbium-171

1. Introduction

The complete separation of all stable Er (Z = 68) isotopes was reported at Oak Ridge National Laboratory in 1958 (SEA 58). Erbium-171 first produced and studied by Cranston (CRA 58), who determined τ = 7.52 h and assigned a Nilsson state [512] 5/2 from a decay-scheme study of the isotope to Tm^{171}.

The g_J value (g_J = - 1.1638) was measured by (SMI 61) by using ${}_{68}Er^{166}$. Cabezas (CAB 60) found the spin 5/2 for Er^{171}, thus supporting Cranston's state assignment and Smith's g_J value. More recently a very accurate value of g_J was obtained from the hfs of Er^{169}(DOY 63), yielding g_J= - 1.16381(5). This last value coincides very well with the prediction of Judd and Lindgren (JUD 61) which used the configuration $(4f)^{12}(6s)^2$ and third-order spin-orbit corrections. The ground-state term is $^3H_6$, as predicted by Hund's rule; the J = 5, 4 states were not observed in the beam.

2. Experiment

A beam of radioactive Er^{171} was produced by bombarding 0.7- to 0.8-g chunks of 99.9%-pure Er metal with thermal neutrons at Vallecitos. Bombardment time of 10 to 12 h was sufficient to give about 1.0 Ci of activity. A steady beam was obtained at approximately 130 W; a run could last 10 to 15 h under good conditions. Due to the short half-life, 15 to 20 h of continuous work was often necessary.

The reaction is

$$Er^{170}(n, \gamma)\, Er^{171} \xrightarrow[\beta^-]{7.5\ h} Tm^{171} \xrightarrow[\beta^-]{1.9\ yr} Yb^{171}.$$

A decay curve taken at the beginning of the investigation (see Fig. IV-12) indicated that more than 90% of the activity belonged to Er^{171}. The possible radioactive contaminants are Er^{163}(τ = 75 min), Er^{165} (τ = 10 h), Er^{169}(τ = 9.4 days) and Tm^{171}(τ = 1.9 yr). The Er^{163} is negligible because of its short half-life, and the Tm^{171} is negligible

because its decay rate (due to its long half-life) is hundreds of times smaller than for Er^{171}. Aside from the fact that Er^{169} has only 1/25 the activity of Er^{171}, its hfs is known and so caused no trouble in the data analysis. The Er^{165}, however, has the same spin ($I = 5/2$) as Er^{171} and therefore has the same g_F factors. The half-lives are similar (7.5 and 10 h) and although the percent abundance and neutron-capture cross section of its parent (Er^{164}) predict it to be 1/50 of the beam, resonances attributable to it were seen. Their amplitude were 1/10 or less than those of Er^{171} and decayed slightly differently. In this way they were separated from the Er^{171} data.

3. Results

A total of 13 resonances were recorded and served to give accurate values of a and b. They are listed in Table IV-3 together with the results of the χ^2 test for both positive and negative values of g_I. The value of g_J used was that quoted in the Er^{169} results (DOY 63); i.e., $g_J = -1.16381(5)$. It should be noted that the frequencies quoted in Table IV-3 are double those used experimentally, because multiple quantum transitions are involved.

The final results are

$$\begin{aligned} a &= \pm 197.0(2.9)\ \text{Mc}, \\ b &= \pm 3646(106)\ \text{Mc}, \\ \frac{b}{a} &> 0. \end{aligned} \tag{4.6}$$

Doyle and Marrus (DOY 63) report for Er^{169}:

$$\begin{aligned} a &= +725.46(31)\text{Mc}, \\ g_I(\text{uncorr}) &= +5.55(27)\times 10^{-4}, \\ \mu_I(\text{corr}) &= +0.513(25)\ \text{nm}. \end{aligned} \tag{4.7}$$

Table IV-3. Erbium-171 resonances and results of χ^2 test (g_I) positive and negative.

g_I	a (Mc)	Δ a (Mc)	b (Mc)	Δb (Mc)	χ^2
positive	196.300	2.163	3622.173	80.456	1.52
negative	197.608	2.213	3669.895	82.169	1.37

ν_K(Mc)	H(G)	ν_{exp}(Mc)	Residual (Mc) $g_I > 0$	Residual (Mc) $g_I < 0$	Transition	Machine
20.000(40)	25.388(45)	58.460(28)	0.009	0.004	α	A
140.000(100)	117.684(58)	272.300(140)	0.137	0.124	α	B
170.000(130)	134.257(69)	310.700(140)	-0.048	-0.060	α	B
215.000(140)	157.118(68)	364.100(140)	0.016	0.007	α	B
249.900(140)	173.694(65)	402.900(140)	0.064	0.058	α	B
410.000(150)	242.716(61)	564.800(200)	-0.149	-0.135	α	B
80.000(100)	79.132(73)	197.500(160)	0.041	0.036	β	B
110.000(100)	99.549(64)	248.940(200)	0.048	0.047	β	B
140.000(100)	117.684(58)	294.900(200)	0.131	0.135	β	B
170.000(150)	134.257(80)	336.900(240)	0.040	0.050	β	B
140.000(100)	117.684(58)	330.850(200)	-0.022	-0.017	γ	B
170.025(150)	134.270(80)	380.000(300)	-0.119	-0.115	γ	B
210.075(150)	154.708(74)	442.400(250)	0.060	0.054	γ	B

Transitions

α	F = 17/2	$m_F = -3/2 \leftrightarrow -7/2$
β	F = 15/2	$m_F = -1/2 \leftrightarrow -5/2$
γ	F = 13/2	$m_F = 1/2 \leftrightarrow -3/2$

By using Eqs. (2.30) and (2.31), together with the Fermi-Segrè relation, Eq. (2.32) and the $\langle 1/r^3 \rangle$ value determined from the above measurements, one calculates

$$\begin{aligned} \mu_I(\text{uncorr}) &= \pm 0.692(48)\ \text{nm}, \\ \mu_I(\text{corr}) &= \pm 0.697(48)\ \text{nm}, \\ Q(\text{uncorr}) &= \mp 2.37(20)\ \text{b}. \end{aligned} \tag{4.8}$$

Equations (4.8) give the nuclear magnetic moment of Er^{171} with and without the diamagnetic shielding correction (RAM 56). However only the uncorrected value of the nuclear quadrupole moment is presented, because of the large uncertainty involved in applying the Sternheimer core-polarization effect (STE 52).

The reliability of Judd and Lindgren's $\langle 1/r^3 \rangle$ is supported by observing that the predictions for μ_I and Q overlap the experimental ones. Using their $\langle 1/r^3 \rangle$, one calculates

$$\begin{aligned} \mu_I(\langle 1/r^3 \rangle) &= \mu_I(\text{corr}) = \pm 0.687(48)\ \text{nm} \\ Q(\text{uncorr}) &= \mp 2.41(20)\ \text{b}. \end{aligned} \tag{4.9}$$

Since the sign of g_I produces no essential difference in χ^2, the final quoted values of a and b are the average of g_I positive and g_I negative. The errors in a and b were chosen to include the outer extremes of both positive and negative g_I.

The ratio b/a causes an inverting of some of the F levels at zero field (BAK 60). The Hamiltonian of an atom at zero field is

$$\mathcal{H}_{hfs} = ha\ I \cdot J + hb \frac{[3(I \cdot J)^2 + 3/2(I \cdot J) - I(I+1)\ J(J+1)]}{2\,I(2I-1)\ J(2J-1)}, \tag{4.10}$$

and letting

$$\begin{aligned} C &= F(F+1) - I(I+1) - J(J+1), \\ \xi &= \frac{b}{a}, \end{aligned} \tag{4.11}$$

one gets for the energy of a state with I, J, and F (in units of ha)

$$W(IJF) = \frac{1}{2}\,C + \frac{3/4\ C(C-1) - I(I+1)\ J(J+1)}{2I(2I-1)\ J(2J-1)}\ \xi. \tag{4.12}$$

For a given I, J, and F the first term and the coefficient of ξ are constants. Therefore W(IJF) plotted with b/a as the abscissa is a straight line whose slope is the coefficient of ξ and has C/2 as its intercept on the energy axis. Now for given values of I and J there is a definite number of associated energy levels F, the ordering of which is dependent on the value of the ratio b/a. The above reference contains graphs and tables showing level orderings for various I, J values as a function of b/a. Figure IV-10 shows the case of I = 5/2, J = 6 (it should be noted that I and J appear symmetrically in Eq. (4.12), so J = 5/2, I = 6 corresponds also to I = 5/2, J = 6), while Table IV-4 gives the critical cross-over points numerically.

Table IV-4. Cross-over points for F levels of system $\binom{I}{J} = 5/2$, $\binom{J}{I} = 6$.

F_i	F_j	$\xi(=\frac{b}{a})$
17/2	15/2	-20.000
17/2	13/2	-30.345
17/2	11/2	-55.000
17/2	9/2	-176.000
17/2	7/2	220.000
15/2	13/2	-73.333
15/2	11/2	880.333
15/2	9/2	73.333
15/2	7/2	41.905
13/2	11/2	55.000
13/2	9/2	32.593
13/2	7/2	24.444
11/2	9/2	22.000
11/2	7/2	17.959
9/2	7/2	14.667

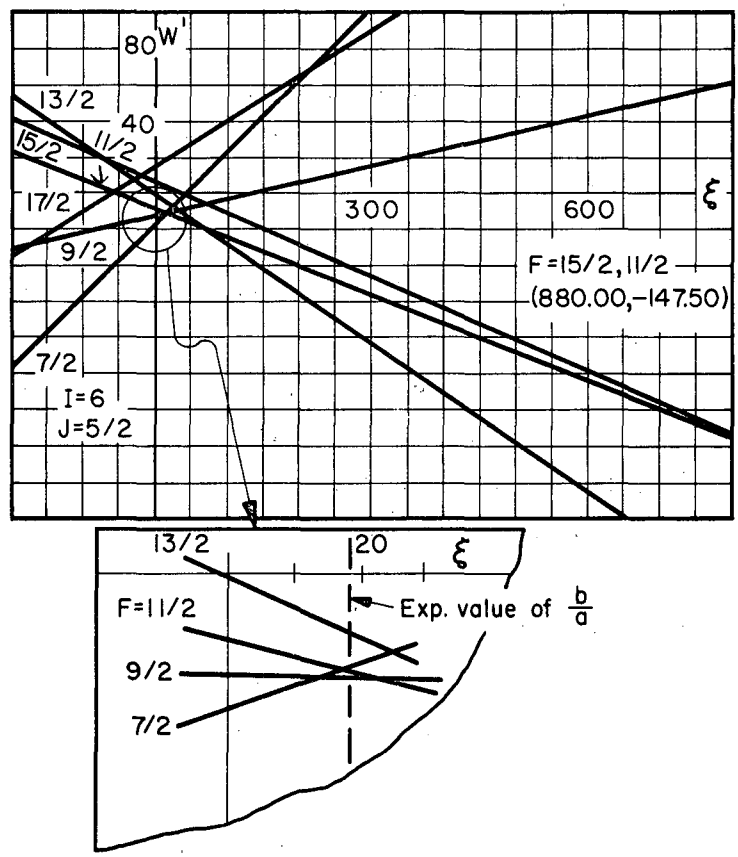

MU-21398-A

Fig. IV-10. Zero-field hfs level ordering for $\binom{I}{J} = 5/2$, $\binom{J}{I} = 6$, as a function of ξ $(= \frac{b}{a})$.

Figure IV-11 shows a schematic hfs diagram for the b/a value found experimentally (b/a≈ 18.5), while Figs. IV-12 through IV-16 are sample resonances and decay plots.

4. Interpretation

Erbium-171 has 68 protons and 103 neutrons in its nucleus. Both types of nucleons are far removed from the nearest closed shells of the shell model (50, 82, 126) so its magnetic-moment and quadrupole-moment predictions are invalid. The shell model does indicate the correct parity in this case (5f, 5/2, π -) though it may not in other collective-model nuclei.

The Nilsson state is [512] 5/2 - so with a knowledge of δ (obtainable from Q) the total collective-model Hamiltonian [Eqs. (2.19) and (2.20), a spin-orbit term, and an $\underset{\sim}{\ell}^2$ term] can be diagonalized by using the harmonic-oscillator representation. An accurate wave function for the last odd particle results from the diagonalization and this, together with an accurate g_R, can be used to predict μ_I. This value, hopefully, agrees with the experimental μ_I.

Using Eqs. (2.24) and (2.25) and the experimentally measured Q, one obtains

$$\delta = 0.238(20), \tag{4.13}$$

which is not too different from the deformations observed in the rare earth region.

To obtain a prediction on μ_I, the $a_{\ell\Omega \pm 1/2}$ values for N = 5 Ω = 5/2 in (MOT 59) were used in Eq. (2.22). The result of this calculation yields

$$\begin{aligned} \mu_I &= -0.95 \text{ nm} \quad ; \quad \eta = 6, \quad \delta \approx 0.3, \\ \mu_I &= -0.91 \text{ nm} \quad ; \quad \eta = 4, \quad \delta \approx 0.2. \end{aligned} \tag{4.14}$$

Although these values lie outside the measured limits on μ_I [μ_I(corr) = ± 0.697(48)nm], they are reasonably close considering one is dealing with 171 particles.

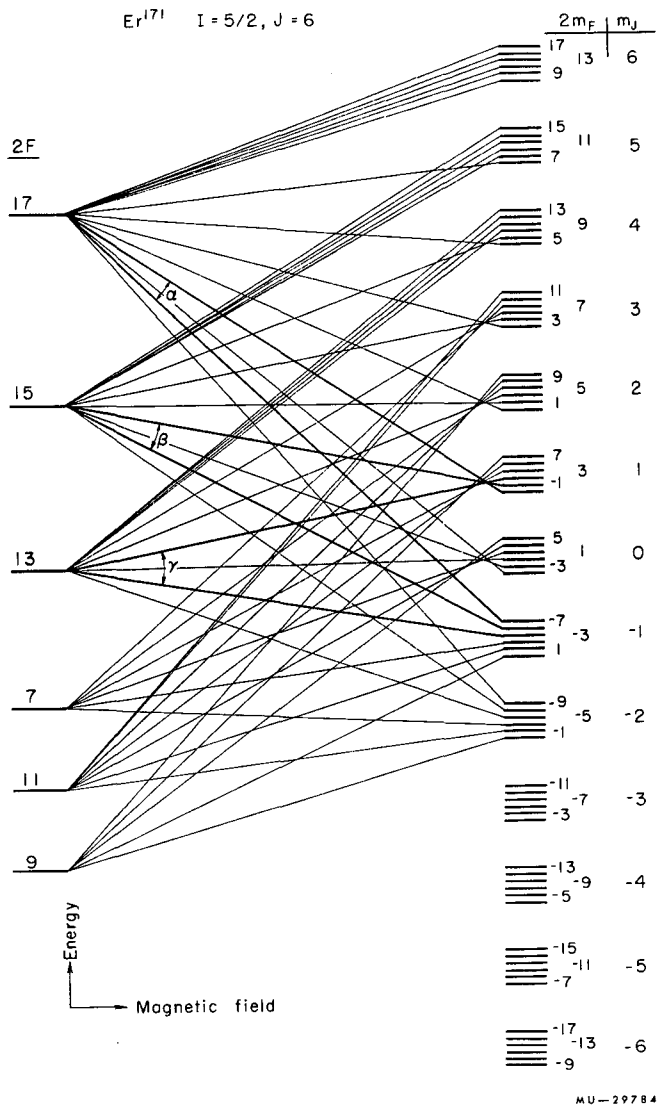

Fig. IV-11. Hyperfine structure diagram (partial schematic) for Er^{171}.

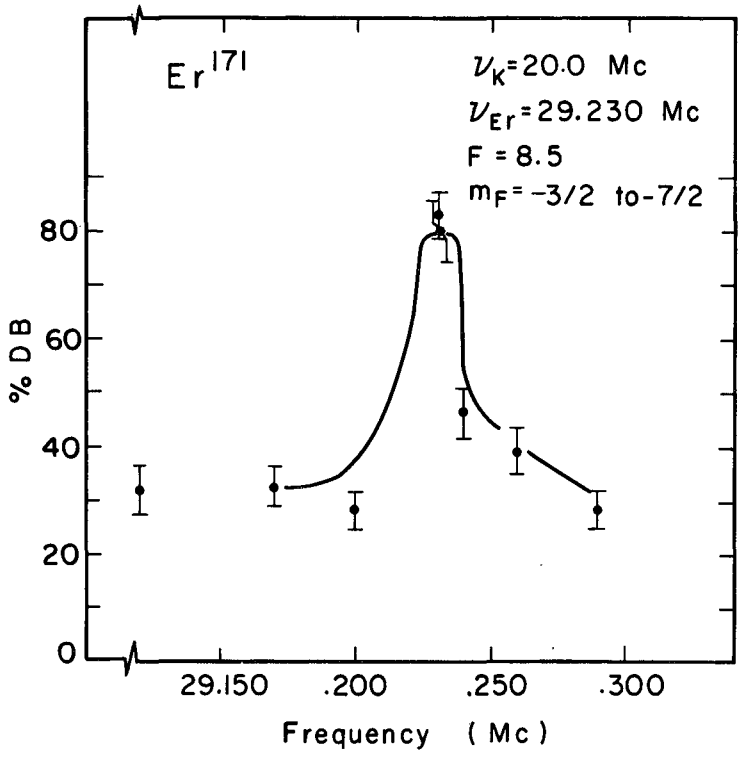

MU-28894

Fig. IV-12. Resonance at ν_K = 20.000 Mc (data taken on machine A). Notice the narrow line width attributable to the uniform C field and also to the characteristic of multiple quantum transitions.

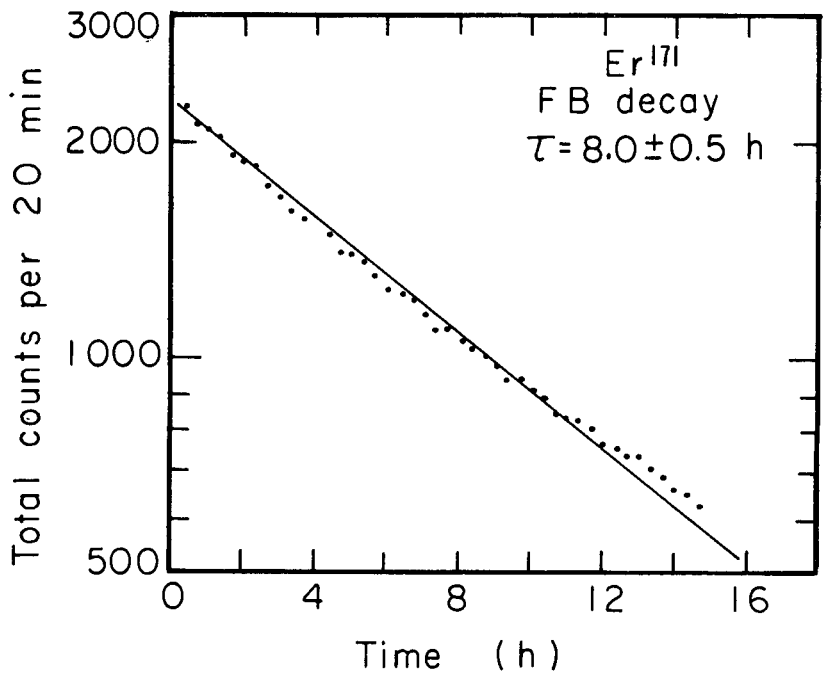

MU-28901

Fig. IV-13. Decay of a full beam (A and B magnets off) of Er^{171}.

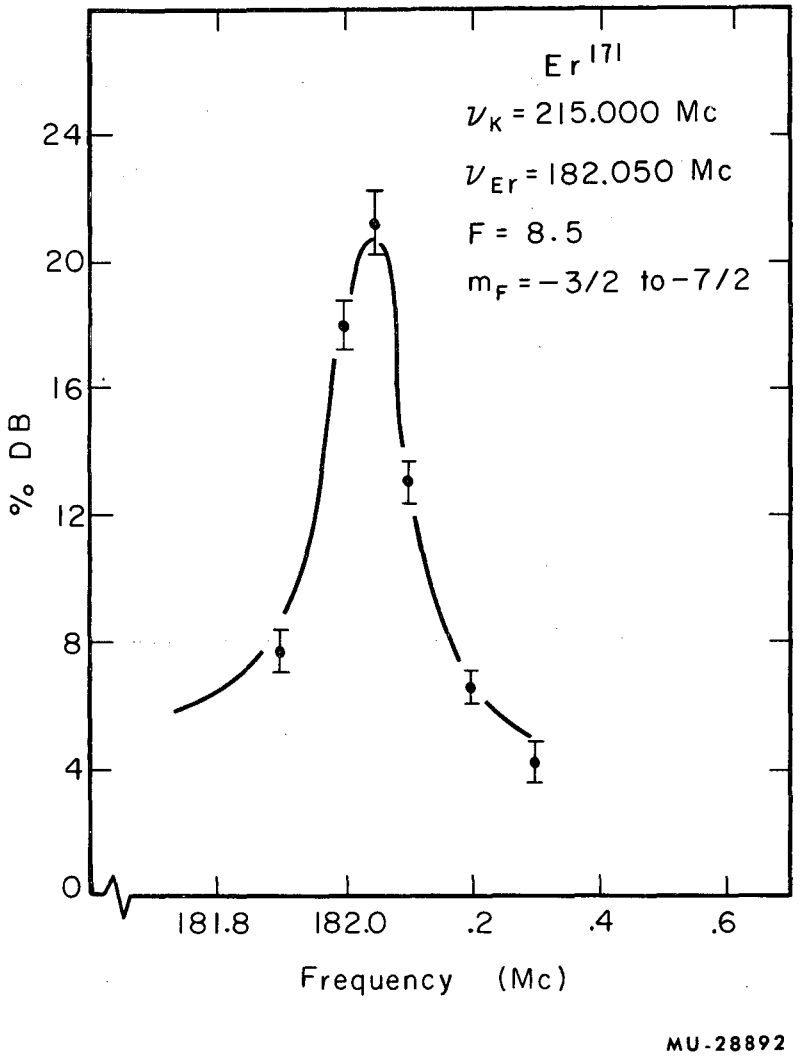

Fig. IV-14. Resonance due to an alpha transition at ν_K = 215.00 Mc (H≈ 157 G).

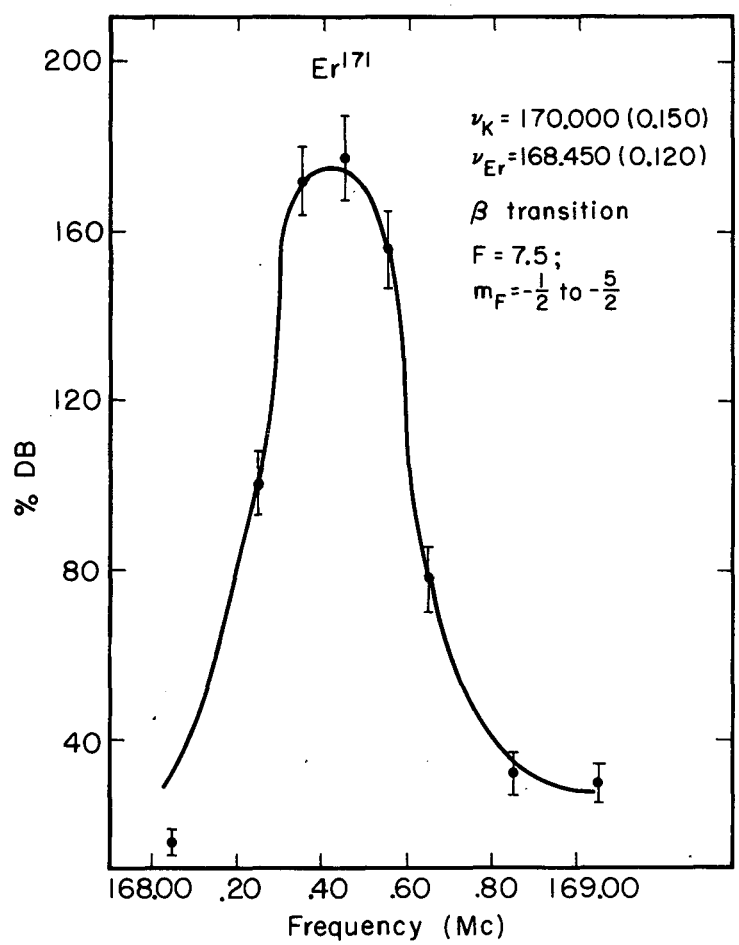

MU-29735

Fig. IV-15. Resonance due to a beta transition at ν_K = 170.000 Mc (H ≈ 134 G).

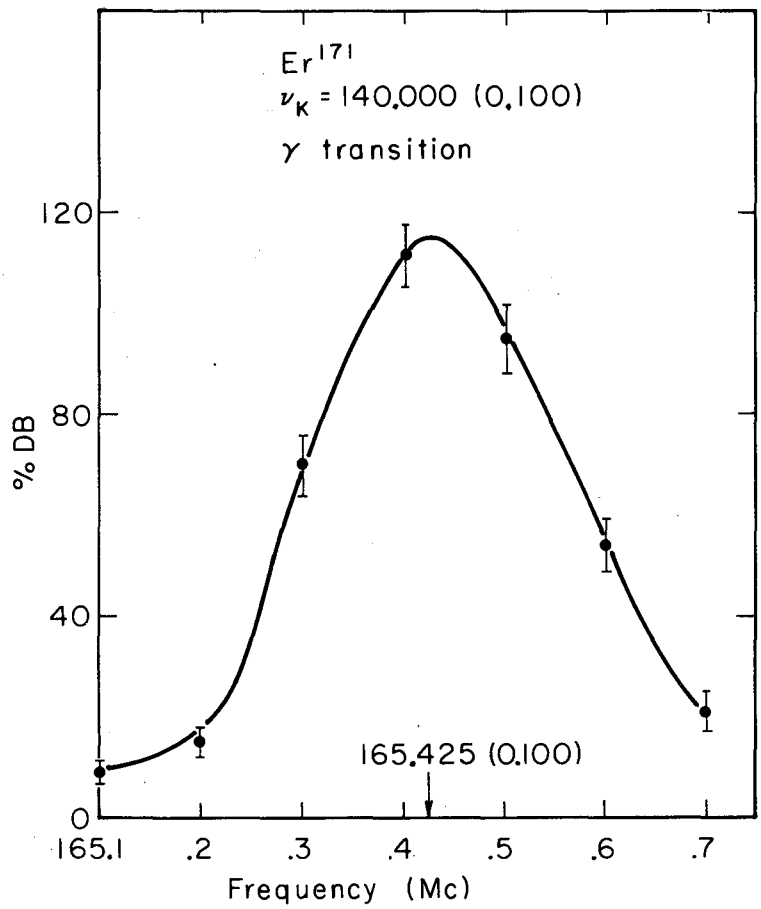

MU—29783

Fig. IV-16. Resonance due to a gamma transition at ν_K = 140.000 Mc (H ≈ 117 G).

The nuclear quadrupole moment in the rare-earth region is usually positive, so coupled with the knowledge that the 4f shell is more than half filled, one can infer that the quadrupole interaction constant is negative. Since $b/a > 0$, the dipole interaction constant is negative also. The resulting sign of μ_I (negative) agrees with that predicted by the collective model. The shell model predicts, as a glance at Table II-1 will show, a positive value for μ_I. In particular, for a $|5f\ 5/2\rangle$ state of a neutron,

$$\begin{aligned} \mu_I &= -\frac{j}{j+1}\,\mu_N, \\ &= -\frac{5}{7}(-1.913) \\ &= +1.366 \text{ nm}. \end{aligned} \tag{4.15}$$

In conclusion,

$$\begin{aligned} &a = \pm\ 197.0(2.9) \text{ Mc}, \\ &\mu_I(\text{corr}) = \pm\ 0.697(48) \text{ nm}, \\ &b = \pm\ 3646.0(106.0) \text{ Mc}, \\ &Q(\text{uncorr}) = \mp\ 2.37(20), \\ &\frac{b}{a} > 0. \end{aligned} \tag{4.16}$$

The deformation $\delta = 0.238(20)$ and μ_I from the collective-model theory is

$$\begin{aligned} \mu_I &= -\ 0.95 \text{ nm} \quad , \quad \delta \approx 0.3, \\ \mu_I &= -\ 0.91 \text{ nm} \quad , \quad \delta \approx 0.2. \end{aligned}$$

If Q is assumed positive, the usual situation in the rare-earth region, then μ_I becomes negative, agreeing in sign with the collective-model prediction. One of the reasons for the predicted moment being outside the limit of the experimental moment is the uncertainty in g_R.

ACKNOWLEDGMENTS

I would like to express my gratitude to the following people for making this work possible:

Professor W. A. Nierenberg for financial support.

Dr. R. Marrus for his guidance throughout the work, his moral support, and, last but not least, his friendship.

Dr. D. McColm for assistance in learning experimental physics.

Professor H. Shugart for his interest and encouragement.

Dr. B. Budick for his generous help during the experiments.

Mr. D. MacDonald for his able engineering skill.

Dr. M. B. White for assistance in running experiments.

The members of the Lawrence Radiation Laboratory Health Chemistry Department for their help in scheduling and handling the radioactive isotopes; in particular, R. McCracken, Mrs. R. Barrett, and P. Van de Mark.

Mr. G. G. Young and his shop staff for fabricating many of the parts required.

Mr. M. Firth for help with the electronic systems.

This work was performed under the auspices of the U. S. Atomic Energy Commission.

APPENDIX

According to Hund's rule, the ground-state term of an atom is one of maximum multiplicity (all electron spins lined up) and afterwards, maximum L consistent with the Pauli principle. A qualitative argument follows:

The total electronic wave function, consisting of a product of spin and space functions, must be antisymmetric. It is possible to have a symmetric spin function and an antisymmetric space function, vice versa, or a mixture of the two (some pairs of electrons with symmetric spins and antisymmetric space functions and other pairs reversed). Since antisymmetric space functions are farther apart then symmetric ones (space quantum numbers are different), the expectation value of $\sum (e^2/r_{ij})$ in the electronic Hamiltonian [Eq. (2.2)] will be minimum if all electron spins are lined up (symmetric spin wave function) and the space wave function is completely antisymmetric. The reason for maximum $\underset{\sim}{L}$ together with maximum multiplicity is less clear; however, the coupling of the two angular momenta to $\underset{\sim}{J}$, the total electronic angular momentum, can be explained via the spin-orbit coupling.

The case for maximum $\underset{\sim}{J}$ if a shell is more than half filled can be explained for equivalent electrons by considering the spin-orbit coupling term in $\mathcal{H}_{\text{electronic}}$ (the next most important term after e^2/r_{ij}) interacting in the state $|LSJ,\ m=J\rangle$. Expressing this state in determinantal product wave functions, one has:

$$(f)^9 \rightarrow {}^6H_{15/2,\cdots 5/2}\,.$$

For $J = |L + S|$;

$$\begin{aligned} |{}^6H,\ 15/2,\ 15/2\rangle &= |5/2, 5/2, 5,\ 5\rangle \ (= |SM_S LM_L\rangle) \\ &= \{\overset{+}{3}\,\overset{+}{2}\,\overset{+}{1}\,\overset{+}{0}\,\overset{+}{-1}\,\overset{+}{-2}\,\overset{+}{-3}\,\overset{-}{3}\,\overset{-}{2}\}\,. \end{aligned} \tag{A-1}$$

Therefore,

$$\left\langle \; -- \; \left|\sum_i \xi(r_i)\underset{\sim}{\ell}_i \cdot \underset{\sim}{s}_i\right| \; -- \; \right\rangle =$$

$$\{\overset{+}{3}\,\overset{+}{2}\,\overset{+}{1}\,\overset{+}{0}\,\overset{+}{-1}\,\overset{+}{-2}\,\overset{-}{-3}\,\overset{-}{2}\}\sum_i \xi(r_i)\underset{\sim}{\ell}_i \cdot \underset{\sim}{s}_i \{\overset{+}{3}\,\overset{+}{2}\,\overset{+}{1}\,\overset{+}{0}\,\overset{+}{-1}\,\overset{+}{-2}\,\overset{-}{-3}\,\overset{-}{2}\}$$

$$= -\frac{3}{2}\,\xi(r) < 0, \tag{A-2}$$

While for $J = |L - S|$,

$$|{}^6H,\ 5/2,\ 5/2\rangle = |5/2,\ -5/2,\ 5,\ 5\rangle$$

$$= \{\overset{-}{3}\,\overset{-}{2}\,\overset{-}{1}\,\overset{-}{0}\,\overset{-}{-1}\,\overset{-}{-2}\,\overset{-}{-3}\,\overset{+}{3}\,\overset{+}{2}\}. \tag{A-3}$$

and so

$$\left\langle \; \left|\sum_i \xi(r_i)\underset{\sim}{\ell}_i \cdot \underset{\sim}{s}_i\right| \; \right\rangle = \{\overset{-}{3}\,\overset{-}{2}\,\overset{-}{1}\,\overset{-}{0}\,\overset{-}{-2}\,\overset{-}{-3}\,\overset{+}{3}\,\overset{+}{2}\}\sum_i \xi(r_i)\underset{\sim}{\ell}_i \cdot \underset{\sim}{s}_i \{\overset{-}{3}\,\overset{-}{2}\,\overset{-}{1}\,\overset{-}{0}\,\overset{-}{-1}\,\overset{-}{-2}\,\overset{-}{-3}\,\overset{+}{3}\,\overset{+}{2}\}$$

$$= \frac{3}{2}\,\xi(r) + \frac{2}{2}\,\xi(r) > 0. \tag{A-4}$$

Bearing in mind that $\xi(r) \approx \frac{1}{r}\frac{\partial V}{\partial r} > 0$, it is reasonable that $\underset{\sim}{J} = |\underset{\sim}{L} + \underset{\sim}{S}|$ lies lowest. For a shell less than half filled the same sort of argument is applicable, yielding $\underset{\sim}{J} = |\underset{\sim}{L} - \underset{\sim}{S}|$.

The author does not mean the above remarks to be a proof of Hund's rule, but rather a sort of rationalization of it.

REFERENCES

ALP 61 S. S. Alpert, The Moments, Spins, and Hyperfine Structures of the Radioactive Isotopes I^{133}, Nd^{141}, Eu^{152}, and Bi^{210} (Ph. D. Thesis), Lawrence Radiation Laboratory Report UCRL-9850, Sept. 1961 (unpublished).

BAK 60 F. M. Baker, Graphs and Tables of Zero Field HFS Level Ordering in Free Atoms, Lawrence Radiation Laboratory Report UCRL-9364, Aug. 1960.

BRE60 M. H. Brennan and A. M. Bernstein, Phys. Rev. 120, 927 (1960).

BLI 57 R. J. Blin-Stoyle, Theories of Nuclear Moments (Oxford University Press, London, 1957).

BRI 57 G. O. Brink, Nuclear Spins of Thallium-197, Thallium-198m, Thallium-199 and Thallium-204 (Ph. D. Thesis), University of California Radiation Laboratory Report UCRL-3642, June 1957 (unpublished).

BOH 53 A. Bohr and B. R. Mottelson, Kgl. Danske Videnskab. Selskab, Mat.-Fys. Medd. 27, No. 16 (1953).

CON 35 E. U. Condon and G. H. Shortley, Theory of Atomic Spectra (Cambridge University Press, London, 1935).

CAB 60 A. Y. Cabezas, Electronic and Nuclear Properties of Some Radioactive Rare-Earth Elements (Ph. D. Thesis), Lawrence Radiation Laboratory Report UCRL-9346 Aug. 1960(unpublished).

CRA 58 F. P. Cranston, Jr., M. E. Bunker, and J. W. Starner, Phys. Rev. 110, 1427 (1958).

DOY 63 W. M. Doyle and R. Marrus, Phys. Rev. (to be published).

FRE 50 M. S. Freedman and D. W. Engelkemein, Phys. Rev. 79, 897 (1950).

GER 62 S. Gerstenkorn (private communication).

HAN 58 P. Gregers Hansen, O. Nathan, O. B. Nielsen, and R. K. Sheline, Nucl. Phys. 6, 630 (1958).

HAR 57 D. R. Hartree, Calculation of Atomic Structures (J. Wiley & Sons, Inc., New York, 1957).

HIL 53 D. L. Hill and J. A. Wheeler, Phys. Rev. 89, 1102 (1953).

HUB 58 J. C. Hubbs, R. Marrus, W. A. Nierenberg, and J. L. Worcester, Phys. Rev. 109, 390 (1958).

JUD 61 B. R. Judd and I. P. K. Lindgren, Phys. Rev. 122, 1802 (1961).

KET 48 B. H. Ketelle and G. E. Boyd, Oak Ridge National Report ORNL-65, July 1948, and ORNL-229, Feb. 1949 (both unpublished).

KED 57 R. W. Kedzie, M. Abraham, and C. D. Jefferies, Phys. Rev. 108, 54 (1957).

MAY 55 M. Goeppert Mayer and J. Hans D. Jensen, Elementary Theory of Nuclear Shell Structure (J. Wiley & Sons, Inc., New York, 1955).

MAR 61 R. A. Marrus and W. A. Nierenberg, On Atomic Beams, in Proceedings of the International School of Physics, Enrico Fermi, Course XVII, August 1960 (Academic Press, New York, 1962), pp. 118-156.

MEG 42 W. F. Meggers, Rev. Mod. Phys. 14, 96 (1942).

MOT 59 B. R. Mottelson and S. G. Nilsson, Kgl. Danske Videnskab. Selskab, Mat.-Fys. Skrifter 1, No. 8 (1959).

NIL 60 S. G. Nilsson, Kgl. Danske Videnskab. Selskab, Mat.-Fys. Medd. 29, No. 16 (1960).

NOR 51 L. A. Nordheim, Rev. Mod. Phys. 23, 322 (1951).

PEN 60 S. Penselin and K. Schlüpmann, University of Heidelberg (private communication to A. Cabezas).

PET 60 F. R. Peterson, Atomic-Beam Research on the Spins, Hyperfine Structures, and Moments of K^{43}, Y^{90}, La^{140}, and Lu^{177} (Ph. D. Thesis), Lawrence Radiation Laboratory Report UCRL-9480, Nov. 1960 (unpublished).

RAM 56 N. F. Ramsey, Molecular Beams (Oxford University Press, New York 1956).

RIT 62 G. R. Ritter, Phys. Rev. 128, 2238 (1962).

SCH 37 T. Schmidt, Z. Physik 106, 358 (1937).

SCH 49 L. I. Schiff, Quantum Mechanics (McGraw-Hill Book Company, Inc., New York 1949).

SEA 58 H. E. Seagren (Isotopes Division), Annual Report of 1957, Oak Ridge National Report ORNL-2492, July 1958.

SMI 56 R. R. Smith, S. D. Reeder, and R. H. Lewis, J. Chem. Phys. 25, 502 (1956).

SMI 57 W. G. Smith, Beta Decay of Tm^{171}, Phys. Rev. 107, 1314 (1957).

SHA 61 B. L. Sharma, Nucl. Phys. 25, 502 (1956).

SMI 61 K. F. Smith and I. J. Spalding, Proc. Roy. Soc. (London) A265, 133 (1961).

STE 52 R. Sternheimer, Phys. Rev. 86, 316 (1952).

WHI 62 M. B. White, Hyperfine Structure and Nuclear Moments of Lu^{176m}, Br^{80}, Br^{80m}, and I^{132} (Ph. D. Thesis), Lawrence Radiation Laboratory Report UCRL-10321, Sept. 1962 (unpublished).

ZAC 42 J. R. Zacharias, Phys. Rev. 61, 270 (1942).

This report was prepared as an account of Government sponsored work. Neither the United States, nor the Commission, nor any person acting on behalf of the Commission:

A. Makes any warranty or representation, expressed or implied, with respect to the accuracy, completeness, or usefulness of the information contained in this report, or that the use of any information, apparatus, method, or process disclosed in this report may not infringe privately owned rights; or

B. Assumes any liabilities with respect to the use of, or for damages resulting from the use of any information, apparatus, method, or process disclosed in this report.

As used in the above, "person acting on behalf of the Commission" includes any employee or contractor of the Commission, or employee of such contractor, to the extent that such employee or contractor of the Commission, or employee of such contractor prepares, disseminates, or provides access to, any information pursuant to his employment or contract with the Commission, or his employment with such contractor.